OCS Study
MMS 2008-030

Survey of Deepwater Currents in the Northwestern Gulf of Mexico

Volume I: Executive Summary

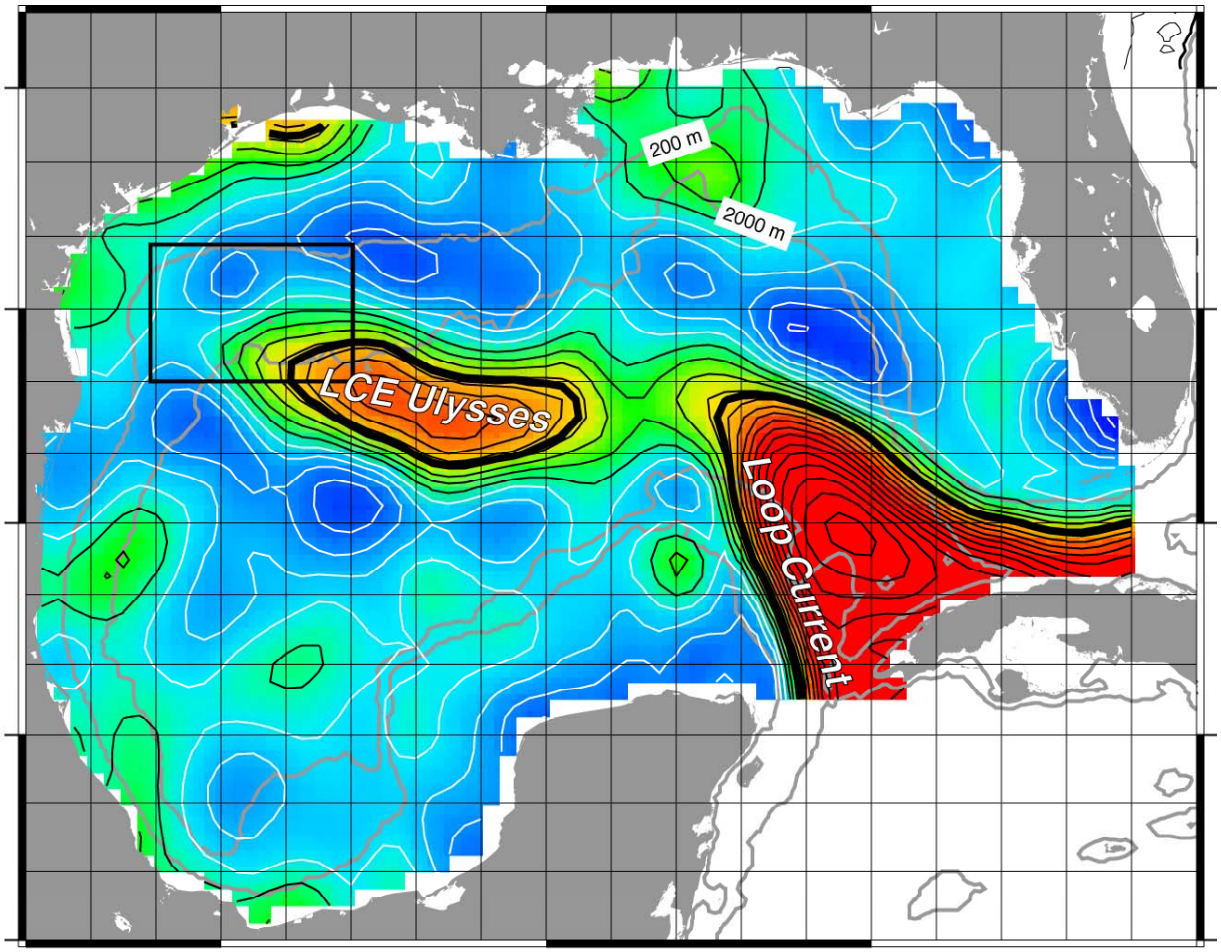

MMS U.S. Department of the Interior
Minerals Management Service
Gulf of Mexico OCS Region

OCS Study
MMS 2008-030

Survey of Deepwater Currents in the Northwestern Gulf of Mexico

Volume I: Executive Summary

Authors

Kathleen Donohue
Peter Hamilton
Robert Leben
Randolph Watts
Evans Waddell

Prepared under MMS Contract
1435-01-03-CT-71562
by
Science Applications International Corporation
615 Oberlin Road, Suite 100
Raleigh, North Carolina 27605

Published by

U.S. Department of the Interior
Minerals Management Service
Gulf of Mexico OCS Region

New Orleans
June 2008

DISCLAIMER

This report was prepared under contract between the Minerals Management Service (MMS) and Science Applications International Corporation. This report has been technically reviewed by the MMS, and it has been approved for publication. Approval does not signify that the contents necessarily reflect the views and policies of the MMS, nor does mention of trade names or commercial products constitute endorsement or recommendation for use. It is, however, exempt from review and compliance with the MMS editorial standards.

REPORT AVAILABILITY

Extra copies of this report may be obtained from the Public Information Office (Mail Stop 5034) at the following address:

U.S. Department of the Interior
Minerals Management Service
Gulf of Mexico OCS Region
Public Information Office (MS 5034)
1201 Elmwood Park Blvd.
New Orleans, LA 70123-2394

Telephone: (504) 736-2519 or
1-800-200-GULF

CITATION

Donohue, K., P. Hamilton, R. Leben, R.Watts, and E. Waddell. 2008. Survey of deepwater currents in the northwestern Gulf of Mexico. Volume I: Executive summary. U.S. Dept. of the Interior, Minerals Management Service, Gulf of Mexico OCS Region, New Orleans, LA. OCS Study MMS 2008-030. 73 pp.

ABOUT THE COVER

The cover shows an image of satellite altimetry that includes the large Loop Current Eddy (LCE) Ulysses just after it had merged with another anticyclone as it entered the southeastern portion of the study area. Although this eddy was never completely within the study area, it and eddies into which it was cleaved had a significant influence on the upper-layer circulation patterns and processes within the northwestern Gulf of Mexico.

ACKNOWLEDGMENT

The support, encouragement and patience of Dr. Alexis Lugo-Fernandez, the MMS COTR, from project inception through completion has been fundamental to the program success and resulting oceanographic insights. Valuable suggestions and support from the Science Review Group (Dr. J. Bane, Dr. William Schmitz and Dr. Wilton Sturges), during the course of the study, were positive, constructive and greatly appreciated. SAIC program personnel, Paul Blankinship (Data Management) and James Singer (Field Operations and Logistics), were crucial to the smooth data support and the outstanding data return and field activities. Mr. G. Chaplin (URI) very successfully conducted all aspects of the PIES instrumentation and field operations. Many additional people, too numerous to identify individually, were important to the program success, e.g., the captains and crews of the *R/V Longhorn* and the *R/V Pelican*. The patience, diligence and expertise of Mrs. Carol Harris in the production of these reports are greatly appreciated by the Program Manager.

TABLE OF CONTENTS

Page

LIST OF FIGURES

LIST OF FIGURES (continued)

LIST OF FIGURES (continued)

LIST OF TABLES

ABBREVIATIONS AND ACRONYMS

ADCP	Acoustic Doppler Current Profiler
APL	Applied Physics Laboratory
AVHRR	Advanced Very High Resolution Radiometer
CCAR	Colorado Center for Astrodynamics Research
CE	Cyclonic Eddy
CEOF	Complex EOF
CERSAT	Centre ERS d'Archivage et de Traitement
CICESE	Centro de Investigacion Cientifica y de Educacion Superior de Ensenada
CNES	Centre National d'Etudes Spatiales, France
CPD	Cycles per Day
CTD (or C/T/D)	Conductivity/Temperature/Depth
CUPOM	University of Colorado – Princeton Ocean Model
DGPS	Digital Global Positioning System
DLP	Day Low Pass
DOF	Degrees of Freedom
EEZ	Exclusive Economic Zone
EKE	Eddy Kinetic Energy
EOF	Empirical Orthogonal Function
ERS-2	Earth Resources Satellite – 2
GDR	Geophysical Data Record
GEM	Gravest Empirical Mode
GEOSAT	Geodetic Satellite
GFO	Geosat Follow-On
GMT	Greenwich Mean Time or UTC
GOM	Gulf of Mexico
GSFC	Goddard Space Flight Center
IES	Inverted Echo Sounder
HBP	Hour Band Pass
HLP	Hour Low Pass
JHU/APL	Johns Hopkins University/Applied Physics Laboratory
KE	Kinetic Energy
LATEX	Louisiana-Texas
LC	Loop Current
LCE	Loop Current Eddy
LCFE	Loop Current Frontal Eddy
LHS	Left Hand Side
LUMCON	Louisiana Universities Marine Consortium
MAB	Meters Above Bottom
MMS	Minerals Management Service
MODIS	Moderate Resolution Imaging Spectroradiometer
NAD	North American Datum
NASA	National Aeronautics and Space Administration
NDBC	National Data Buoy Center
NESDIS	National Environmental Satellite, Data, and Information Service

NOAA	National Oceanic and Atmospheric Administration
OA	Objective Analysis
PDR	Precision Depth Recorder
PI	Principal Investigator
PIES	Inverted Echo Sounder with Pressure
PNG	Portable Network Graphics
PO.DAAC	Physical Oceanography Distributed Active Archive Center
PSU	Practical Salinity Unit
PV	Potential Vorticity
RAFOS	Ranging and Fixing of Sound (SOFAR spelled backwards)
RFP	Request for Proposal
RHS	Right Hand Side
RMS	Route Mean Square
SAIC	Science Applications International Corporation
SCULP	Surface Current and Lagrangian-drift Program
SeaWiFS	Sea-viewing Wide Field-of-view Sensor
SNR	Signal-to-Noise Ratio
SSH	Sea Surface Height
SSHA	Sea Surface Height Anomaly
SST	Sea Surface Temperature
SUW	Subtropical Underwater
T	Temperature
TABS	Texas Automated Buoy System
TAMU	Texas A&M University
T/C/P	Temperature/Conductivity/Pressure
TOPEX/Poseidon	Ocean Topography Experiment
TOP/POS	TOPEX/Poseidon
T/P	Temperature/Pressure
TRW	Topographic Rossby Wave
T/S	Temperature/Salinity
T/P/S	Temperature/Pressure/Salinity
T/S/P	Temperature/Salinity/Pressure
UNOLS	University-National Oceanographic Laboratory System
UTC	Coordinated Universal Time or GMT
UTMSI	University of Texas Marine Science Institute
WGS	World Geodetic System

CHAPTER 1 INTRODUCTION AND OBJECTIVES

1.1 Background

The Minerals Management Service (MMS) awarded a contract to Science Applications International Corporation (SAIC) to conduct a study titled: *Survey of Deepwater Currents in the Northwestern Gulf of Mexico* (often referred to as the NW Gulf Study). The timing and general area of investigation extends the focus of a series of preliminary studies that as a group will provide a basis for effective design and implementation of comprehensive ocean investigations having a goal of in-depth understanding and characterization of Gulf of Mexico (GOM) circulation and dynamics. These prior MMS-funded studies include the Deepwater Physical Oceanography Reanalysis and Synthesis of Historical Data (Nowlin, et al., 2001), the DeSoto Canyon Eddy Intrusion Study (Hamilton, et al., 2000), the Study of Deepwater Observations in the Northern Gulf of Mexico from In-Situ Current Meters and PIES (Hamilton, et al., 2003), and the recently completed Exploratory Study of Deepwater Currents in the GOM (Donohue, et al., 2006). Additionally, the MMS is presently funding a field measurement/data synthesis program titled: *A Study of Deepwater Currents in the Eastern Gulf of Mexico*. Clearly, the NW Gulf Study should be viewed in the context of an expanding multi-program database that is providing insights to initial characterization of dynamical aspects of the GOM circulation patterns that vary significantly in both time and space.

For the MMS, this NW Gulf Study was one component of concurrent MMS-funded measurement efforts in the western GOM. Support was provided separately by the MMS for measurements in an American Sector and a Mexican Sector. (The program in the Mexican Sector was funded by the MMS through an agreement with CICESE.) The dividing line between the sectors was the Exclusive Economic Zone (EEZ) boundary between the United States and the Republic of Mexico (Figure 1-1). The MMS coordinated the timing and placement of instrumentation so observations would be mutually compatible, and hence, support a combined or integrated data analysis and process synthesis.

Boundaries of the American Sector of NW Gulf Study area are shown in Figure 1-1 which also identifies selected major and relevant bathymetric and cultural features. Within this American Sector, the Sigsbee Escarpment is a major bathymetric feature that has a substantial influence on various dynamic ocean processes (Donohue, et al., 2006). It is apparent in this figure that within the American Sector, the area of deeper water (depths greater than ~ 2500 m) at the base of the Sigsbee Escarpment is relatively limited. However, within the contiguous Mexican Sector, there are extensive areas of deepwater below the base of the Sigsbee Escarpment and its extension on the western margin of the GOM, the Perdido Escarpment. In the American Sector, the western and northern study area boundaries were defined by the 200-m isobath. Hence, the focus of measurements and processes of interest are those that occur on and over the continental slope and upper rise in the northwestern corner of the GOM.

The MMS-specified objectives for this study are:

A. To collect current ocean data to increase our deepwater database and knowledge of the deep circulation in the northwestern GOM;

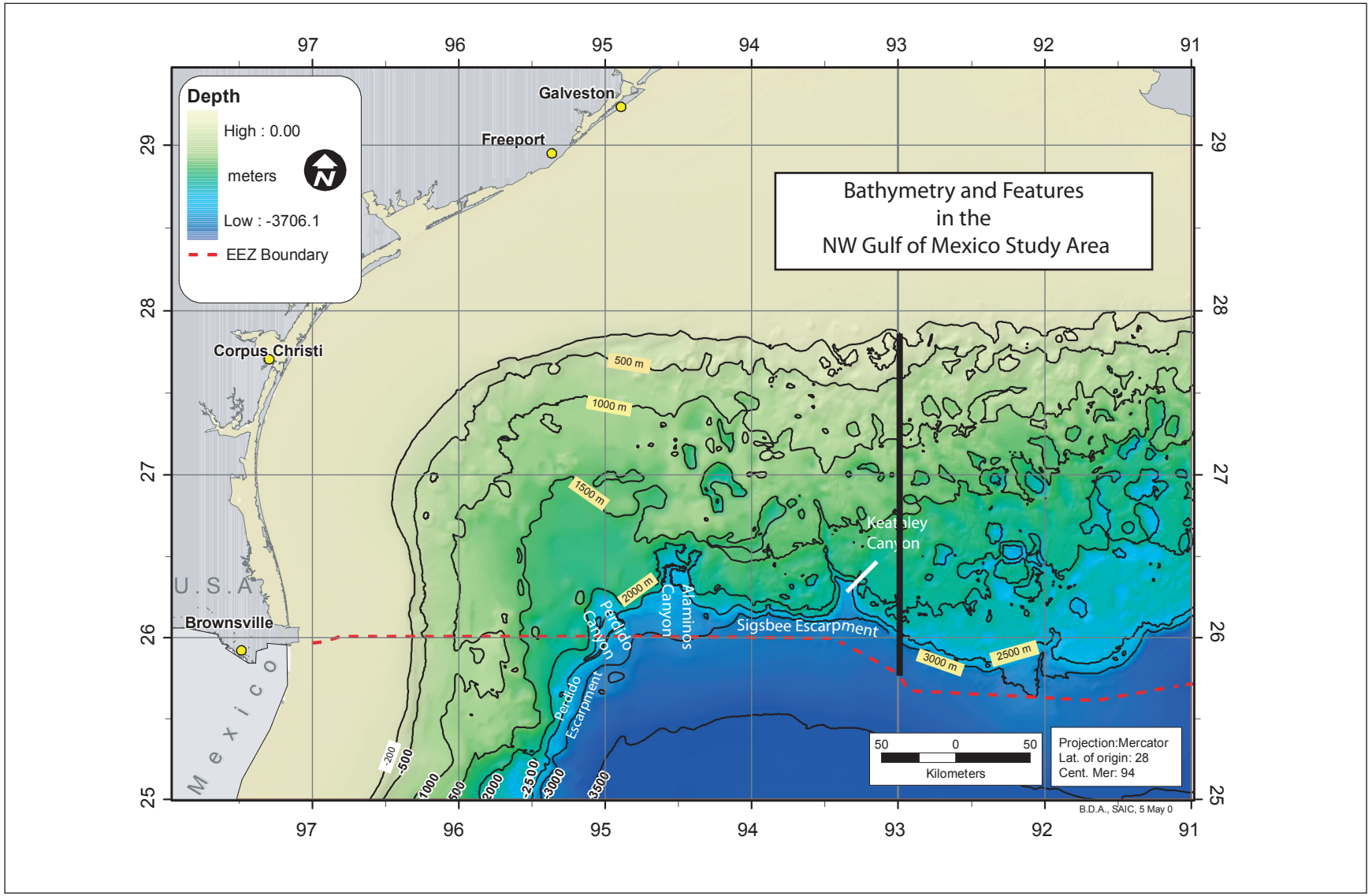

Figure 1-1. Complex bathymetry and key bottom features within the NW Gulf Study area (American Sector). This study area eastern boundary is 93°W. The western and northern boundaries are the 200-m isobath. The southern boundary is the EEZ. Note, in this map area the Sigsbee Escarpment extends to the east of the study area along the 2500-m and 3000-m isobaths.

B. To gather information to estimate oceanographic parameters needed to make experimental designs of full-scale physical oceanography studies in deepwater; and

C. To provide information to use in oil spill analyses including the emerging deep spill analysis, other ongoing studies, to help evaluate exploration plans, and contribute to the preparation of NEPA documents.

1.2 General Program Description

As identified in the Request for Proposal (RFP), a possible design for the study involved 13 full-depth moorings instrumented with various and appropriate sensors to resolve and estimate key parameters and conditions within the study area. Additionally, a combination of remotely sensed (satellite) data types (e.g., altimetry, radiometry, and color) were to be acquired and used to aid in the interpretation of mesoscale features and physical data in the study area. Within the scope of work for this study, there was a specification for coordination of all activities with oceanographers from Mexico who were responsible for Mexican Sector activities and data.

Using direct and acoustic current sensors, various temperature and salinity sensors, and remote sensing, the SAIC team of scientists and engineers designed an innovative, data rich, and observationally integrated field measurement program that supported all of the program objectives (Figure 1-2). As an Option in its original proposal, SAIC recommended that MMS support use of Inverted Echo Sounders with Pressure (PIES) as part of an integrated field measurement program. PIES had proven to provide valuable and cost-effective information for resolving both upper and lower-layer baroclinic and barotropic processes when used as part of the Exploratory Study (Donohue, et al., 2006). When MMS exercised the PIES option, the initial observations on the moored arrays were supplemented with PIES placed at locations that used the PIES and existing moorings to create an observational program that resolved key ocean parameters and patterns at finer spatial scales. In addition, selected hydrocasts were made to support calibration of the PIES observations.

As proposed, PIES in conjunction with conventional current meter moorings provided the following key cost-effective design enhancements:

- Time series of full-depth temperature and salinity profiles at the 13 PIES sites over the study area (See PIES locations relative to mooring locations in Figure 1-2).

- Substantially broader and better resolved time varying, 3-D coverage of the temperature and salinity structure than was possible with 13 conventional moorings.

- Bottom-pressure measurements at 10 PIES sites to help map deep eddies and help distinguish between deep eddies and topographic Rossby waves (TRWs).

- An analytical method in conjunction with PIES observations for determining the baroclinic and barotropic bottom pressure contributions to altimeter measurements of sea surface height (SSH).

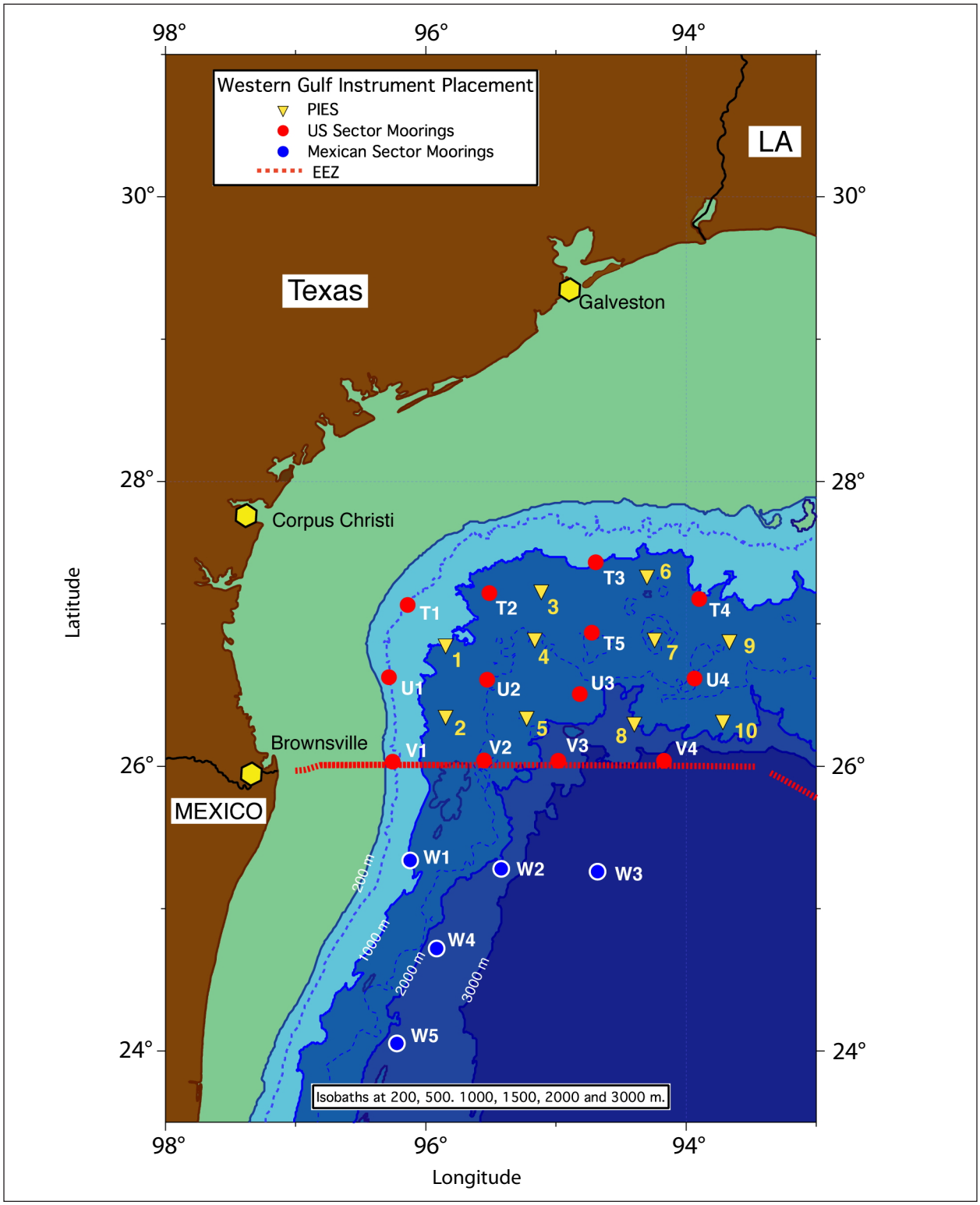

Figure 1-2. Locations of moorings and PIES in the American and Mexican Sectors. The red line indicates the international EEZ boundary.

1.3 General Program Schedule

The general schedule of field measurements and data gathering activities is shown in Figure 1-3. The contract was awarded in October 2003 with mobilization occurring over the first six months. As originally designed, initial deployment of moorings occurred in late March 2004 with rotation to have occurred in September 2004 and recovery in March 2005. With a goal of having the most overlap with PIES and the observations in the Mexican Sector, the mooring rotation cruise was conducted in early October and the recovery in August 2005 for a total mooring deployment interval of 15 months. Approval of the PIES option and associated implementation resulted in the PIES being deployed in October 2004 and recovered in early August 2005. Moorings in the Mexican Sector were deployed in September 2004 and recovered in October/November 2005. The overlap of American Sector moorings and Mexican Sector moorings was approximately 10 months. Satellite imagery was obtained and processed to document conditions and support observations in both the American and Mexican Sectors – approximately from February 2004 through September 2005.

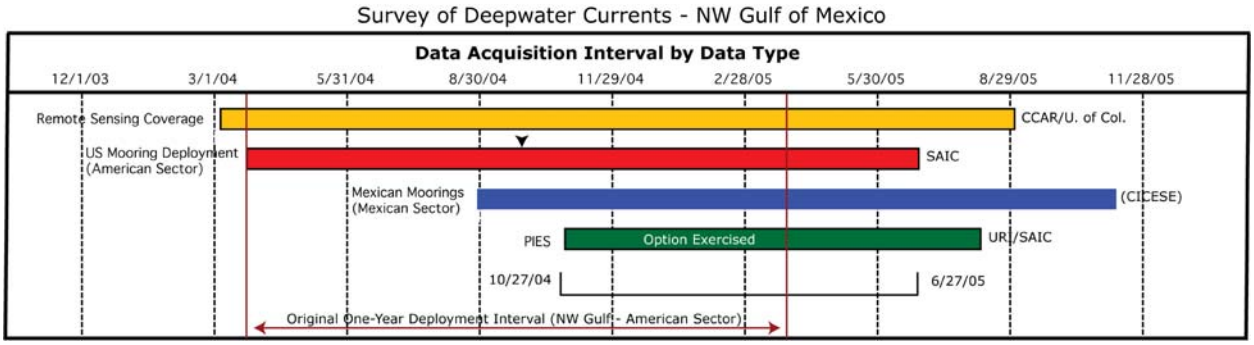

Figure 1-3. Schedule and relationship of various data types collected and used in this study.

1.4 Study Participants

Presented below are Science Team/Principal Investigators (PIs) who contributed to the analyses and subsequent writing of this report. Also shown are the primary SAIC personnel who supported the project. Note that the PIs were supported in their various activities by scientists and engineers at their home institutions. These additional support personnel were essential to the success of all aspects of the study from observations to analyses to graphics production.

Science Team and associated primary, but not sole, measurement responsibility:

PIES

Dr. Kathleen Donohue, University of Rhode Island

Dr. Randolph Watts, University of Rhode Island

Remote Sensing

Dr. Robert Leben, University of Colorado

In-situ Current Measurements

Dr. Peter Hamilton, SAIC

It is important to note that the complete and comprehensive data set from the American and Mexican Sectors was available to each of the members of the Science Team. In conjunction with this approach, there was considerable collegial interaction so that combined expertise was brought to bear on the complex processes occurring in the upper and lower layers of the water column in the study areas.

The Science Team was supported by Management and Logistics personnel as follows:

Dr. Evans Waddell - Program Manager

Mr. James Singer - Logistics Manager and Cruise Chief Scientist

Mr. Paul Blankinship - Data Manager

All moored current-meter arrays were the responsibility of SAIC. PIs from the University of Rhode Island was responsible for PIES instrumentation, including building, preparation, deployment and recovery. Satellite remote sensing was the responsibility of the PI from the University of Colorado.

1.5 Report Organization

This report provides a description of processes occurring in the upper and lower layers of the northwestern GOM during the field measurement interval. In support of this goal, report chapters include:

Chapter 1: Introduction that describes the general context and content of the study.

Chapter 2: Experimental Design and Methodology that briefly describes measurements made and observations used in the study.

Chapter 3: Upper-Ocean Circulation.

Chapter 4: Deep Circulation.

Chapter 5: High-Frequency Currents.

Chapter 6: Recommendations.

CHAPTER 2 METHODOLOGY

Moored Arrays

Key field measurements were made using instrumented moorings placed at the locations indicated in Figure1-2. Full-depth mooring instrumentation was of two configurations: those on the 500-m isobath and those in deeper water. The types and placement of equipment is shown in Table 2-1. As seen in this table, ADCPs were placed near the top of all full-depth moorings. Those on the 500-m isobath had 300-kHz units at 90-m depth and those in deeper water had 75-kHz units at 450-m depth. The ADCPs provided estimates of the horizontal velocity profile from just above the instrument to 10 to 40 m below the water surface. As shown in Table 2-1, all moorings had temperature and/or conductivity sensors placed above the upper ADCP. In deep water, currents were measured at 250-m intervals above 1000 m and at 500 m intervals below 1000 m. On each mooring a current meter was placed 100 m above the local bottom. This general instrument placement reflects the objectives of the program in conjunction with the experience the program PIs had gained in prior deep GOM studies. Data return from moored instruments over the intervals shown in Figure 2-1a-e was 97% and the PIES had almost 100% data return (4 months of bottom pressure were missing). As a result of the excellent performance of all sensors, an outstanding and comprehensive database was available to the PIs in developing a sound characterization of ocean conditions in the study area.

PIES

At locations shown in Figure 1-2, an array of ten inverted echo sounders with pressure gauges (PIES) were deployed. The PIES is a bottom-mounted instrument that emits 12-kHz sound pulses and measures the round-trip travel times of these acoustic pulses from sea floor to sea surface and back. The PIES were also equipped with an extremely accurate pressure gauge to measure bottom pressure. A detailed description of instrument and initial processing may be found in Hamilton et al. (2003) and Donohue et al. (2006) with key steps described below.

The array of PIES combined with measurements from the full-depth (tall) moorings enabled a quantitative mapping of the regional circulation. Round-trip acoustic travel time measured by the inverted echo sounder, allowed estimates of vertical profiles of temperature, salinity, and density, utilizing empirical relationships established with historical hydrography. We also used these relationships to convert the tall moorings into pseudo inverted echo sounders (IES). Pressure was leveled using mean measured current measurements at the full-depth moorings. Deep pressure records combined with estimated horizontal density gradients yielded referenced geostrophic velocities. With this array, 4-D maps of temperature, salinity, density, and velocity 3-spatial dimensions and time were produced. The tall moorings were recovered in late June 2005, therefore, circulation maps were created for nearly eight months.

Table 2-1a

Mooring locations and moored instrument levels for the NW Gulf of Mexico Program with nominal mooring and instrument depths (Moorings T1-T5)

NW GULF OF MEXICO (03/19/04 - 07/03/05)				
Mooring	**Location**	**Water Depth (M)**	**Instrument Depth (M) (MAB)**	**Instrument Type (Serial No.)**
T1	27°07.823'N 96°08.133'W 27.130°N 96.136°N	500	75 90/UP 90 150 250 350 450 (50)	TEMP (D591) 300 KHz ADCP (197) (209) T/P (M6159) T/S/P (1719) (2696) S4 (08111780) (07801678) TEMP (T1153) S4 (04020660) (08111779)
T2	27°13.144'N 95°30.935'W 27.219°N 95.516°W	1200	75 150 194 [2]/UP 194 [2] 250 350 450/UP 458 [2] 750 750 1100 (100)	TEMP (D585) T/S/P (1342) 300 KHz ADCP (1200) T/P (M4670) TEMP (T1267) TEMP (T1154) 75 KHz ADCP (4887) (4888) RCM-11 (359) S4 (08111746) (08582010) T/P (M6160) (M4663) RCM-11 (349) (355)
T3	27°24.669'N 94°40.184'W 27.411°N 94.670°W	1000	75 150 250 350 450/UP 750 750 900 (100)	TEMP (D593) T/S/P (2693) (2695) TEMP (T1270) TEMP (T1155) 75 KHz ADCP (4913) S4 (08291851) (08111750) T/P (M6164) RCM-11 (348) (350)
T4	27°09.867'N 93°54.157'W 27.164°N 93.903°W	1000	75 150 194 [1]/UP 194 [1] 250 350 450/UP 458 [1] 750 750 [2] 900 (100)	TEMP (D614) T/S/P (3387) (3391) 300 KHz ADCP (214) T/P (M6166) TEMP (T1271) TEMP (T1156) 75 KHz ADCP (4888) (924) RCM-7 (11389) S4 (08161758) (08161755) T/P (M6166) RCM-11 (356) RCM-7 (11791)
T5	26°55.425'N 94°43.387'W 26.924°N 94.723°W	1500	75 150 194 [2] 250 350 450/UP 750 750 1000 1400 (100)	TEMP (D597) T/S/P (3388) RCM-11 (354) TEMP (T1275) TEMP (T1157) 75 KHz ADCP (4855) S4 (08111750) (08111746) T/P (M6161) RCM-7/8 (6922) (10533) RCM-11 (350) (349)

MAB = Meters Above Bottom.
[ ] = Deployed during indicated deployment only.

Table 2-1b

Mooring locations and moored instrument levels for the NW Gulf of Mexico Program with nominal mooring and instrument depths (Moorings U1-U4, V1-V2)

NW GULF OF MEXICO (03/19/04 - 07/03/05)				
Mooring	**Location**	**Water Depth (M)**	**Instrument Depth (M) (MAB)**	**Instrument Type (Serial No.)**
U1	26°37.408'N 96°16.958'W 26.623°N 96.283°W	500	75 90/UP 90 150 250 350 450 (50)	TEMP (D583) 300 KHz ADCP (1200) (197) T/P (M6163) T/S/P (1720) (2694) S4 (08582010) (07961709) TEMP (T1158) S4 (07961708) (04020660)
U2	26°37.511'N 95°32.818'W 26.625°N 95.547°W	1500	75 150 250 350 450/UP 750 750 1000 1400 (100)	TEMP (D595) T/S/P (3389) TEMP (T1276) TEMP (T1159) 75 KHz ADCP (4918) S4 (07961709) (07961708) T/P (M6162) RCM-7/8 (9950) (12788) RCM-11 (352)
U3	26°30.413'N 94°48.684'W 26.507°N 94.811°W	1700	75 150 250 350 450/UP 750 1000 1600 (100)	TEMP (D617) T/S/P (3390) TEMP (T1277) TEMP (T439) 75 KHz ADCP (4914) (4856) RCM-11 (360) (364) RCM-8 (10533) (12789) RCM-7 (9949) (10350)
U4	26°37.077'N 93°55.692'W 26.618°N 93.928°W	1500	75 150 250 350 450/UP 750 1000 1400 (100)	TEMP (D620) T/S/P (3391) (3387) TEMP (T1278) TEMP (T1160) 75 KHz ADCP (4866) RCM-11 (361) RCM-7 (9524) RCM-7 (10350) (10881) RCM-11 (353) RCM-8 (12804)
V1	26°02.023'N 96°15.153'W 26.034°N 96.253°W	500	75 90/UP 90 150 250 350 450 (50)	TEMP (D581) 300 KHz ADCP (209) (214) T/P (M6158) T/S/P (1341) S4 (07801678) (08161757) TEMP (T1162) S4 (08111779) (08161758)
V2	26°02.849'N 95°35.024'W 26.047°N 95.584°W	1500	75 150 250 350 450/UP 750 1000 1400 (100)	TEMP (D621) T/S/P (3392) TEMP (T1279) (C943) TEMP (T442) 75 KHz ADCP (4865) RCM-11 (362) (360) RCM-7/8 (9948) (7582) RCM-11 (354) (351)

MAB = Meters Above Bottom.

Table 2-1c

Mooring locations and moored instrument levels for the NW Gulf of Mexico Program with nominal mooring and instrument depths Moorings V3 and V4)

NW GULF OF MEXICO (03/19/04 - 07/03/05)				
Mooring	**Location**	**Water Depth (M)**	**Instrument Depth (M) (MAB)**	**Instrument Type (Serial No.)**
V3	26°02.868'N 94°57.019'W 26.048°N 94.950°W	2500	75 150 250 350 450/UP 750 1000 1500 2000 2400 (100)	TEMP (D633) T/S/P (3393) TEMP (T1280) TEMP (T440) 75 KHz ADCP (4856) (4914) RCM-11 (363) RCM-7 (9985) (11450) RCM-7 (6892) RCM-11 (351) (357) RCM-11 (355) (358)
V4	26°02.182'N 94°05.614'W 26.036°N 94.094°W	3100	75 150 250 350 450/UP 750 1000 1500 2000 2500 3000 (100)	TEMP (D634) T/S/P (3394) TEMP (T1187) TEMP (T441) 75 KHz ADCP (4817) RCM-11(364) (361) RCM-7 (9636) (11432) RCM-8 (7582) (7528) RCM-11 (357) RCM-8 (12806) RCM-11 (358) (356) RCM-11 (359) (353)

MAB = Meters Above Bottom.

Three tall moorings (T5, U2, and U3) embedded in the middle of the array provided measurements to evaluate PIES-derived fields of temperature. Comparison sites around the periphery of the mapping grid were excluded from this comparison. The temperatures compare well (Figures 2-3 through 2-4). Differences derive from the GEM parameterization, from mapping uncertainty was instrument errors (both mooring and PIES). The 450-m temperature records were used to convert moorings to pseudo IES observations; the comparisons indicate how well the GEM look-up describes the temperature structure.

A more stringent test of the GEM/PIES mapping methodology is the comparison with measured velocities since the PIES velocities are 2nd-order quantities determined via differentiation. Again, the agreement between measured and PIES-estimated series was good (Figures 2-5 through 2-7). Here the T5, U2, and U3 comparisons are shown in Figure 2-5 through Figure 2-7. Again, both series track each other well. Offsets are likely due to uncertainty in the absolute pressure of moorings. Here mapping error plays a larger role in the discrepancy between the two time series; mapped current will differ from point-measured current when features have small scales relative to the array grid. For example, the mid-water column jet at T5 near day 420 is not resolved by the PIES array.

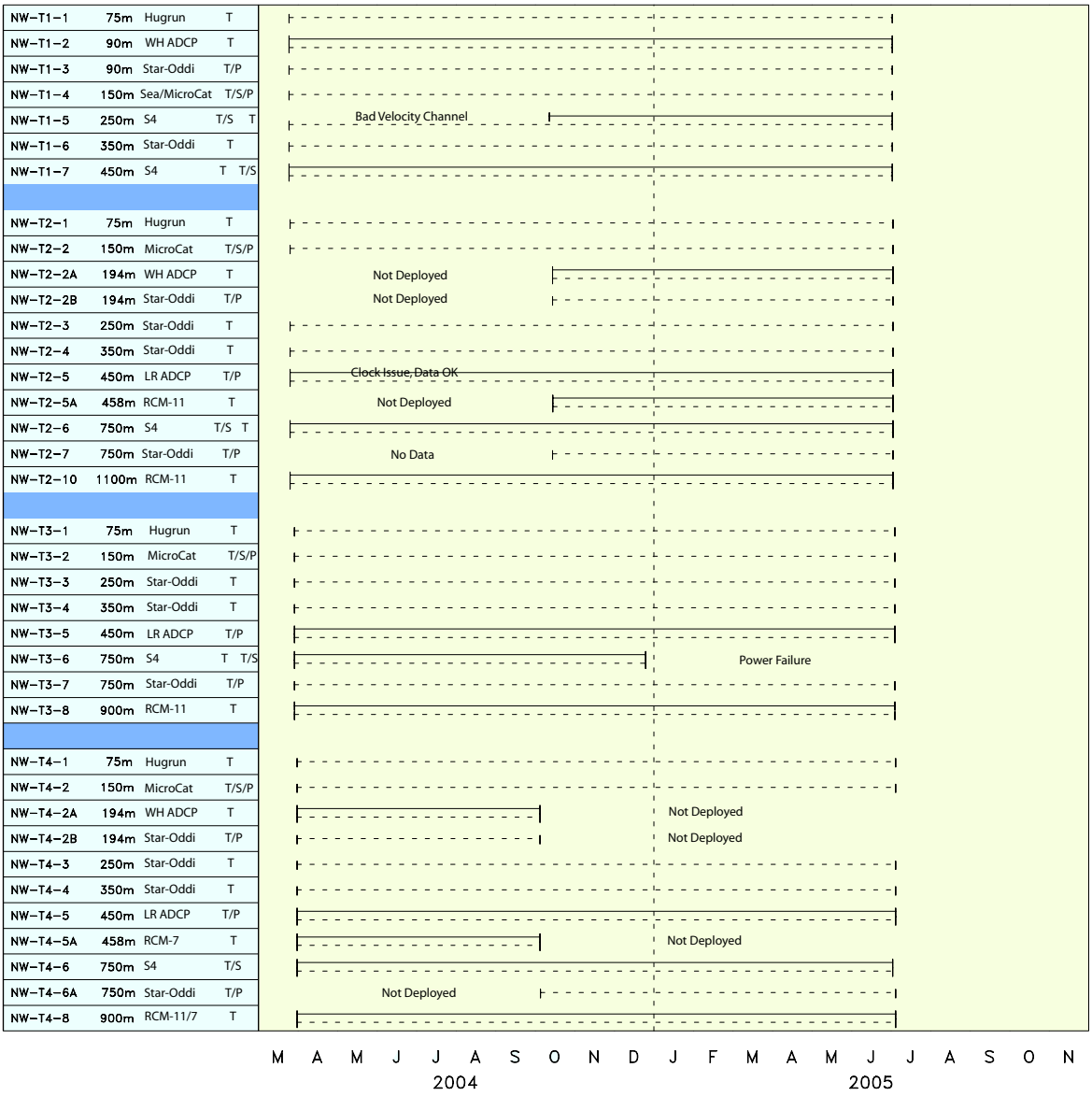

Figure 2-1a. Timeline of instrument on Moorings T1, T2, T3 and T4. Shown in addition to the instrument/measurment ID is the instrument type, placement depth, variables measured and when deployed. Instruments are numbered down from the upper instrument on a mooring line. “Not Deployed” indications are for instruments deployed for shorter intervals to provide comparison (hopefully redundant) information relative to longer term instrument deployments.

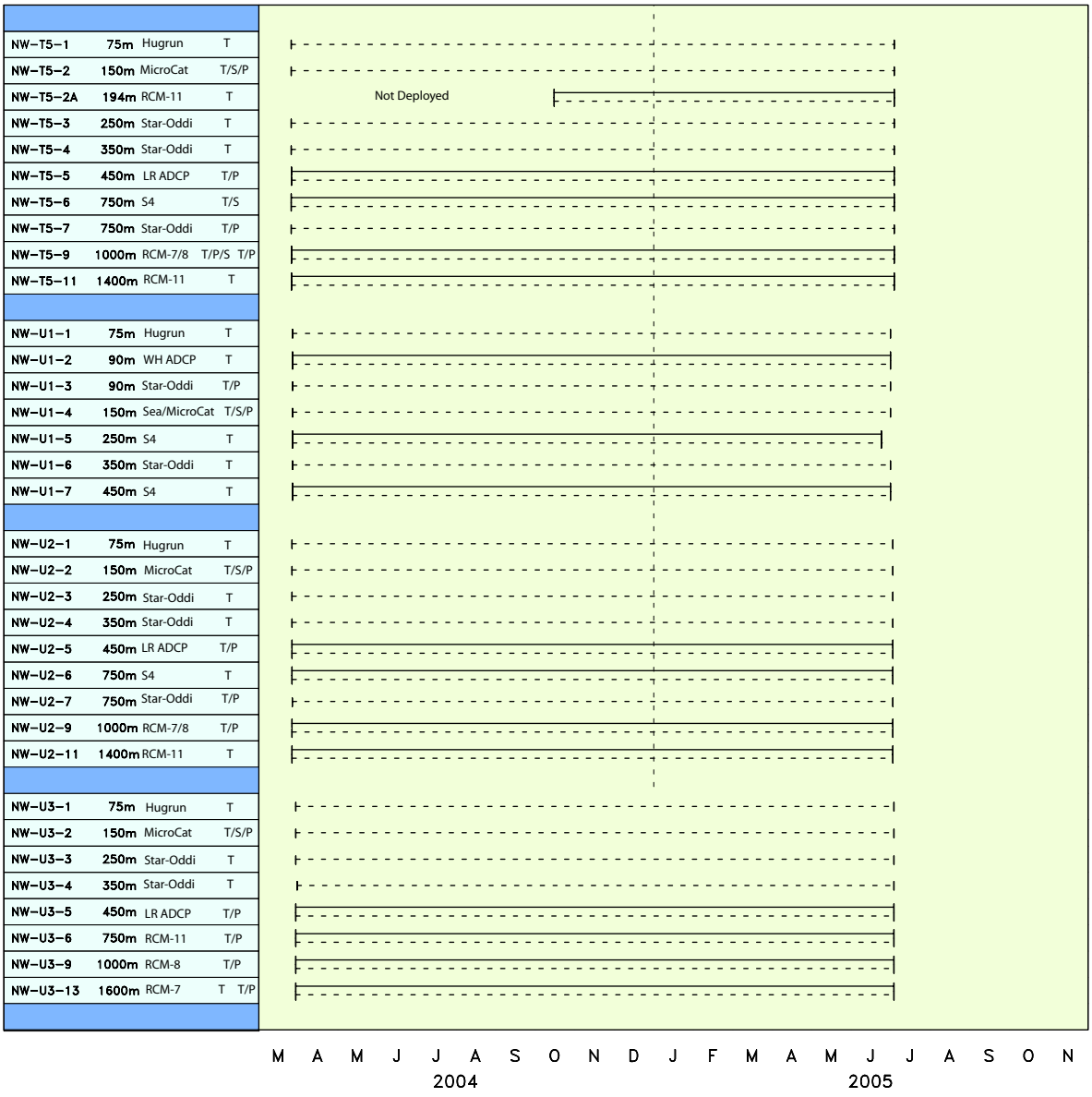

Figure 2-1b. Timeline of instrument on Moorings T5, U1, U2 and U3. Shown in addition to the instrument/measurment ID is the instrument type, placement depth, variables measured and when deployed. Instruments are numbered down from the upper instrument on a mooring line. "Not Deployed" indications are for instruments deployed for shorter intervals to provide comparison (hopefully redundant) information relative to longer term instrument deployments.

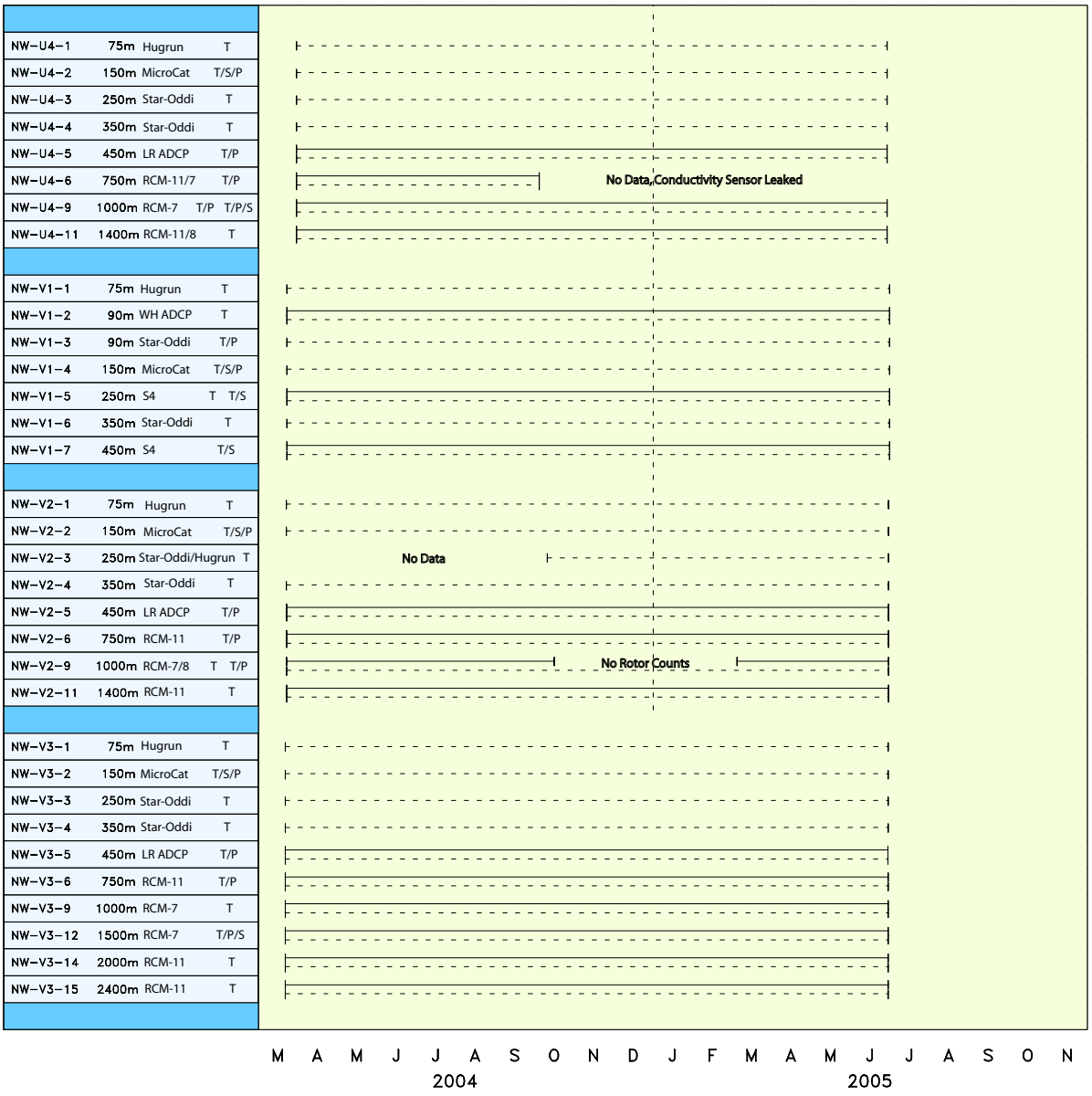

Figure 2-1c. Timeline of instrument on Moorings U4, V1, V2 and V3. Shown in addition to the instrument/measurment ID is the instrument type, placement depth, variables measured and when deployed. Instruments are numbered down from the upper instrument on a mooring line.

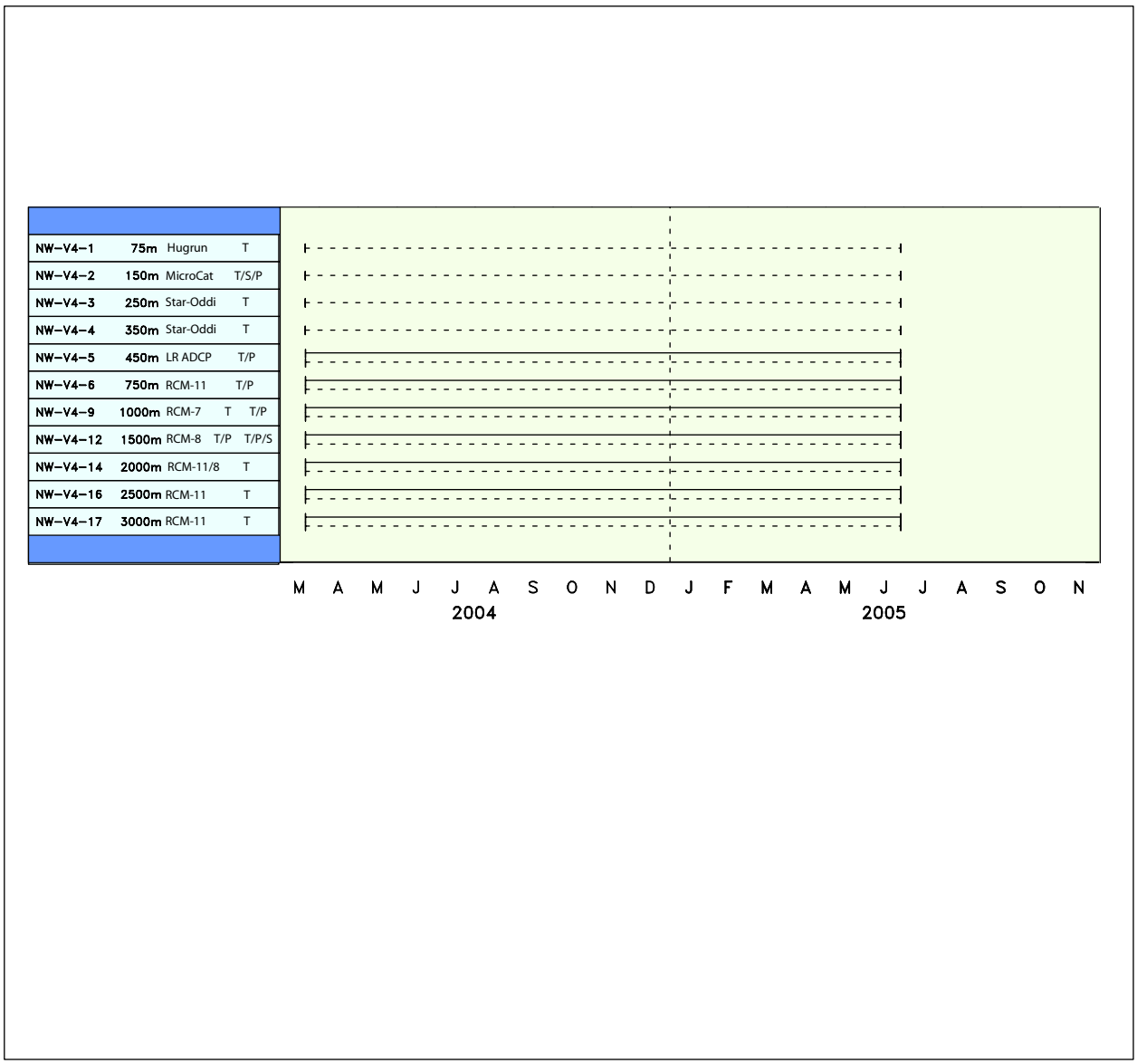

Figure 2-1d. Timeline of instrument on Mooring V4. Shown in addition to the instrument/ measurment ID is the instrument type, placement depth, variables measured and when deployed. Instruments are numbered down from the upper instrument on a mooring line.

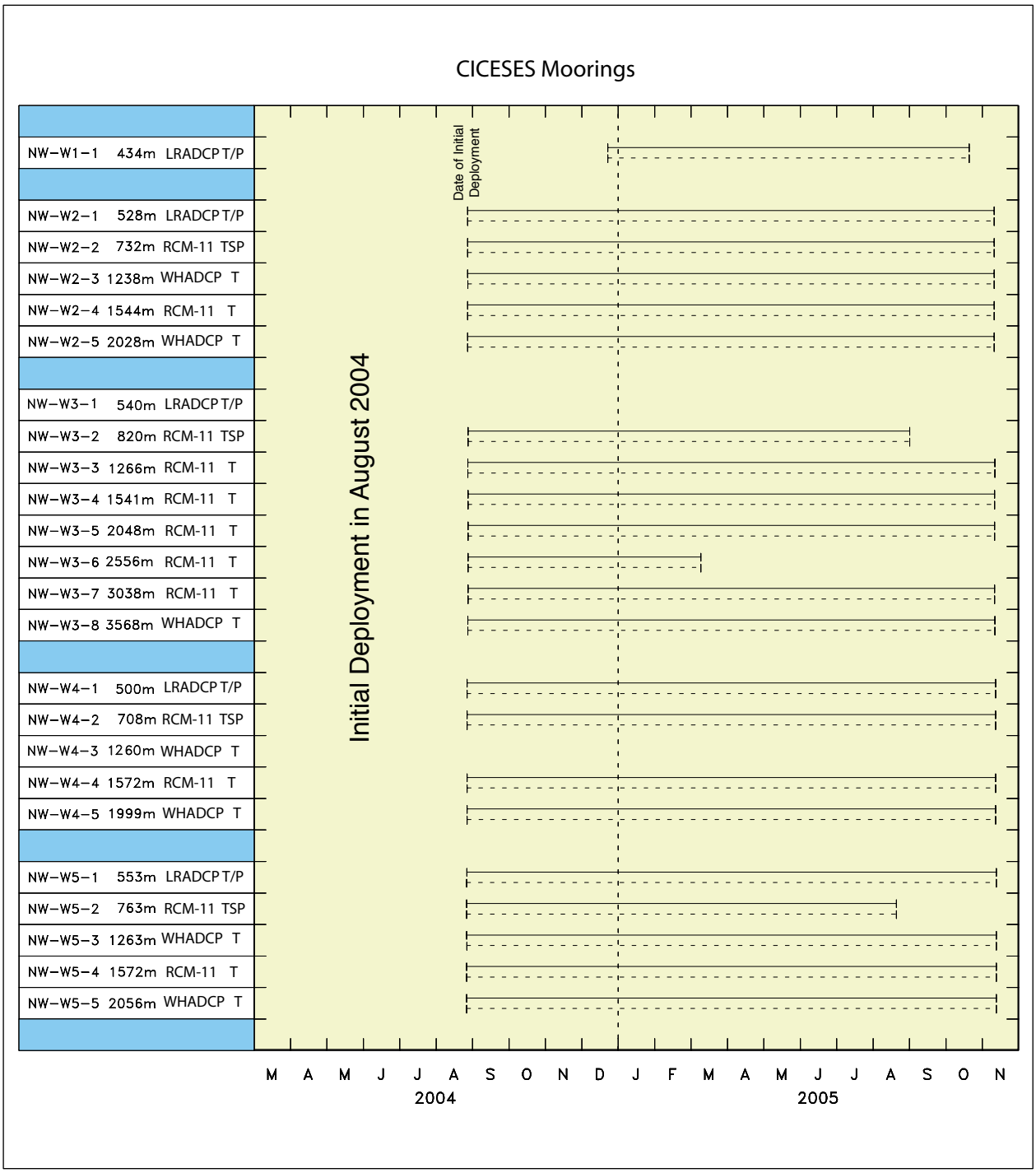

Figure 2-1e. Timeline of instrument on Moorings W1-W5 that were deployed by CICESE in the Mexican sector of the MMS-funded field measurement program. Shown in addition to the instrument/measurment ID is the instrument type, placement depth, variables measured and when deployed. Instruments are numbered down from the upper instrument on a mooring line. The mooring and instrument numbering scheme used by CICESE may differ from that used above.

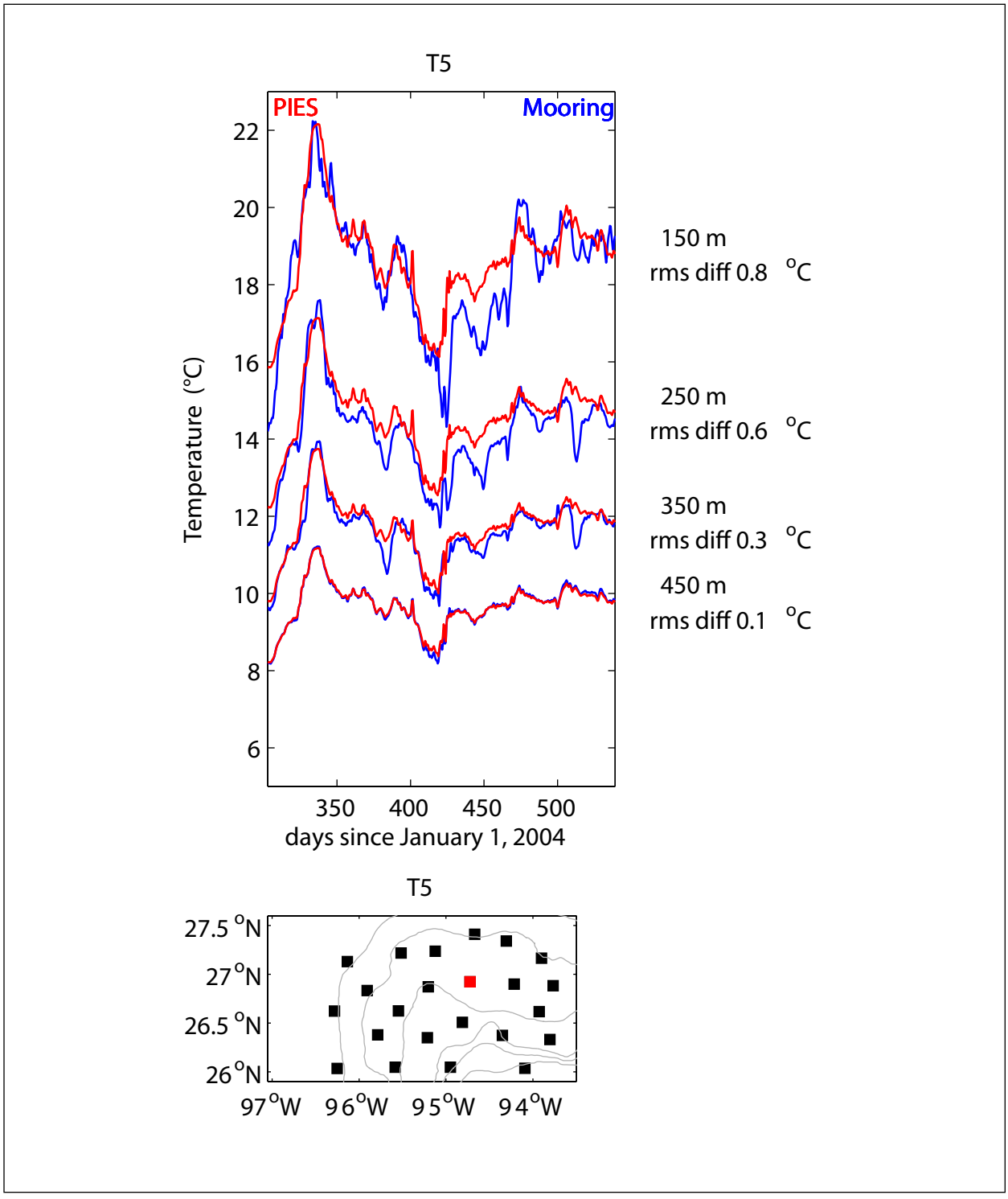

Figure 2-2. Comparison between the T5 mooring (blue) and PIES-derived (red) temperature. The nominal depth and rms difference between PIES and the T5 mooring are noted to the right of each series. The bottom panel shows the location of the PIES (black) and pseudo-IES (black) and the T5 mooring (red). Bathymetry contoured every 500 m.

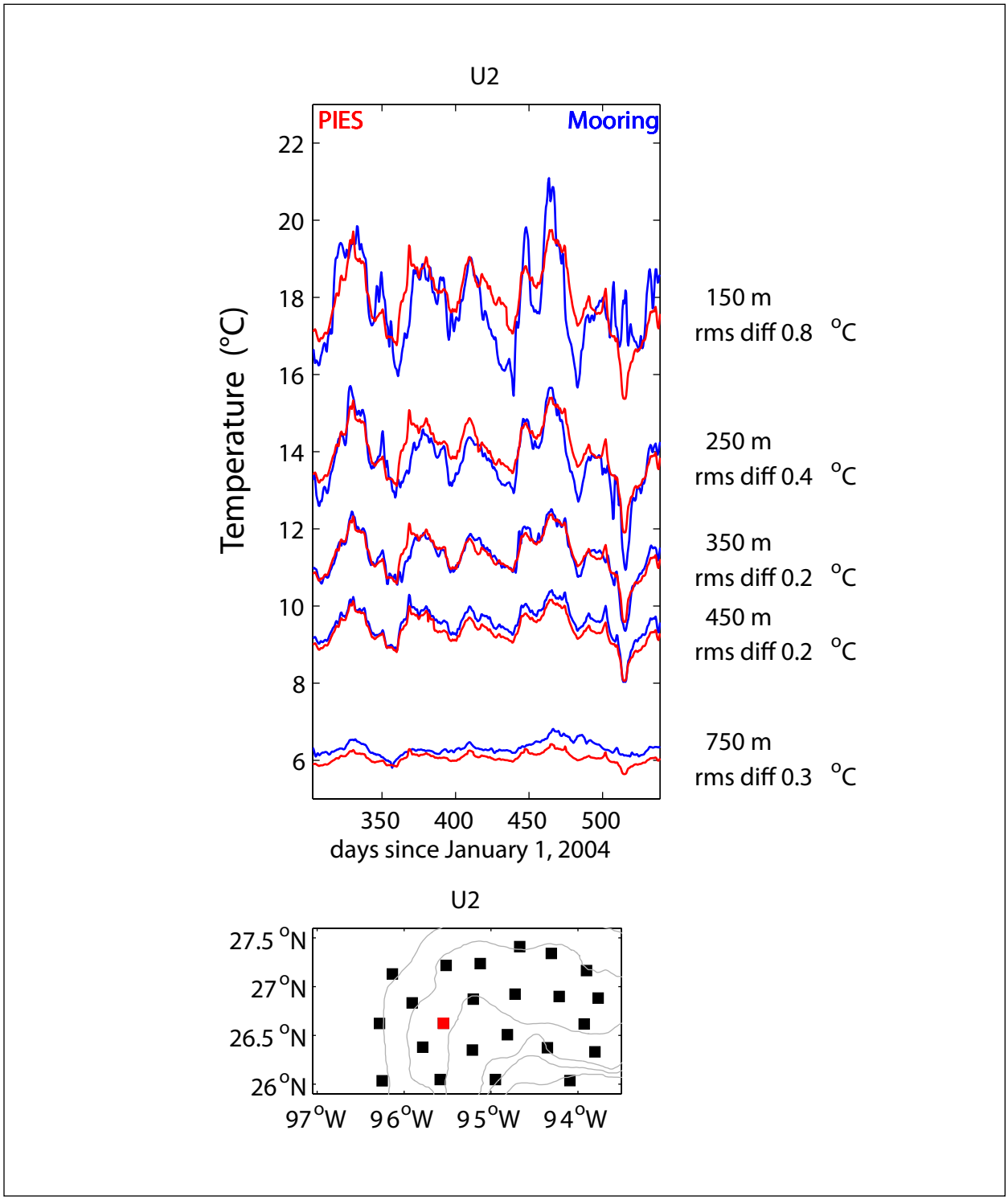

Figure 2-3. Comparison between the U2 mooring (blue) and PIES-derived (red) temperature. The nominal depth and rms difference between PIES and the U2 mooring are noted to the right of each series. The bottom panel shows the location of the PIES (black) and pseudo-IES (black) and the U2 mooring (red). Bathymetry contoured every 500 m.

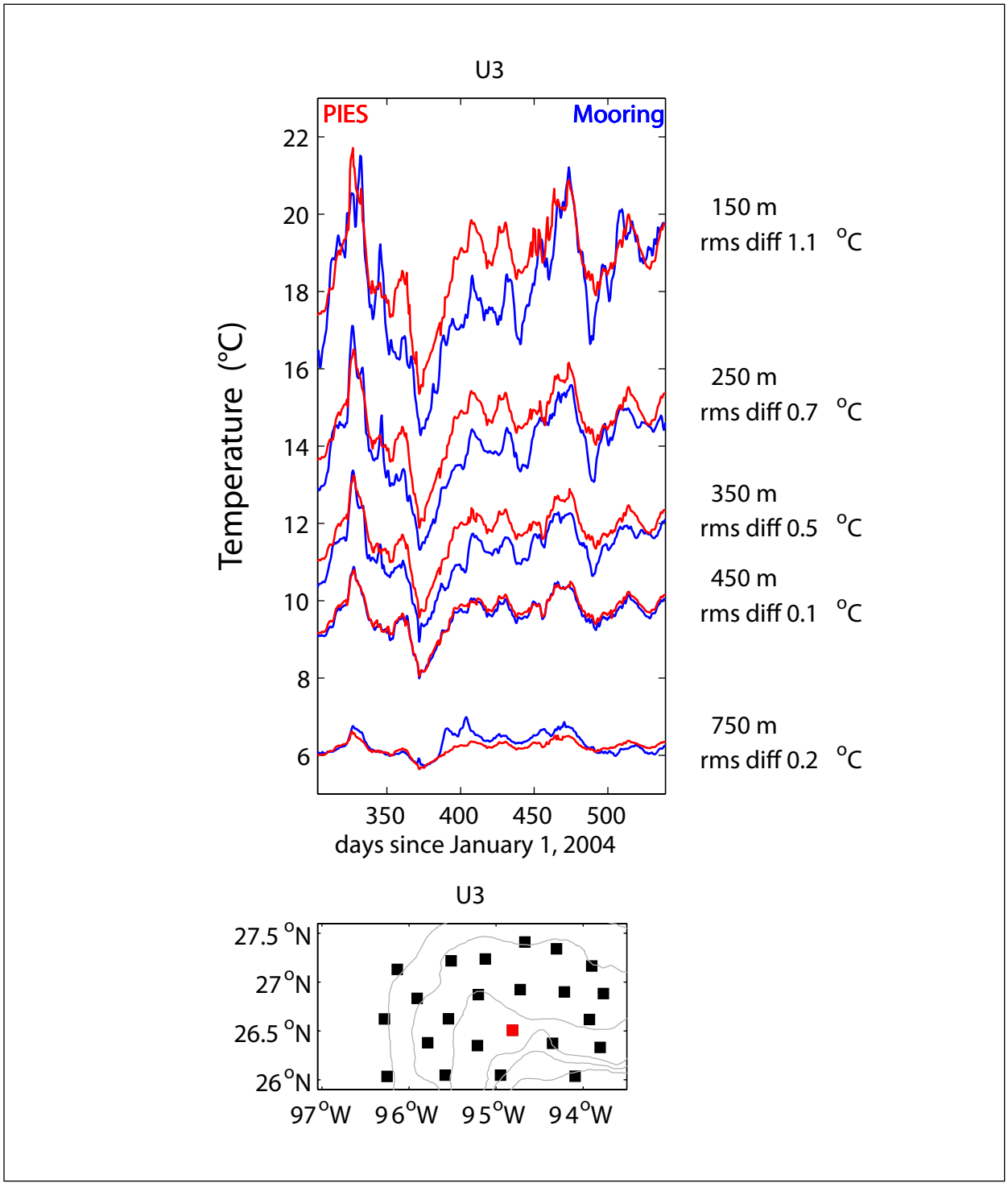

Figure 2-4. Comparison between the U3 mooring (blue) and PIES-derived (red) temperature. The nominal depth and rms difference between PIES and the U3 mooring are noted to the right of each series. The bottom panel shows the location of the PIES (black) and pseudo-IES (black) and the U3 mooring (red). Bathymetry contoured every 500 m.

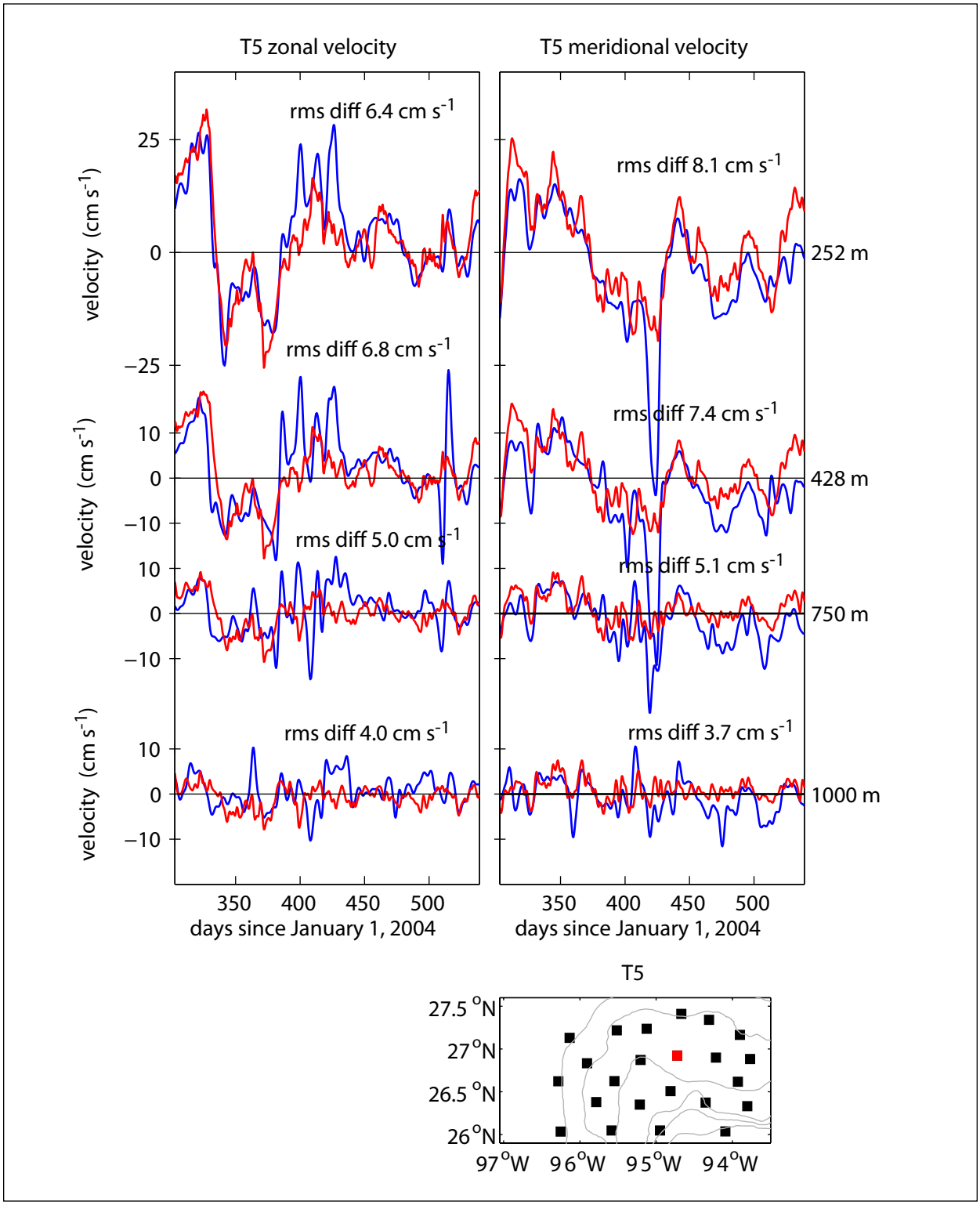

Figure 2-5. Comparison between the T5 mooring (blue) and PIES-derived (red) zonal (left) and meridional (right) velocities. The nominal depth and rms difference between PIES and the T5 mooring are noted to the right of each series. The bottom panel shows the location of the PIES (black) and pseudo-IES (black) and the T5 mooring (red). Bathymetry contoured every 500-m depth.

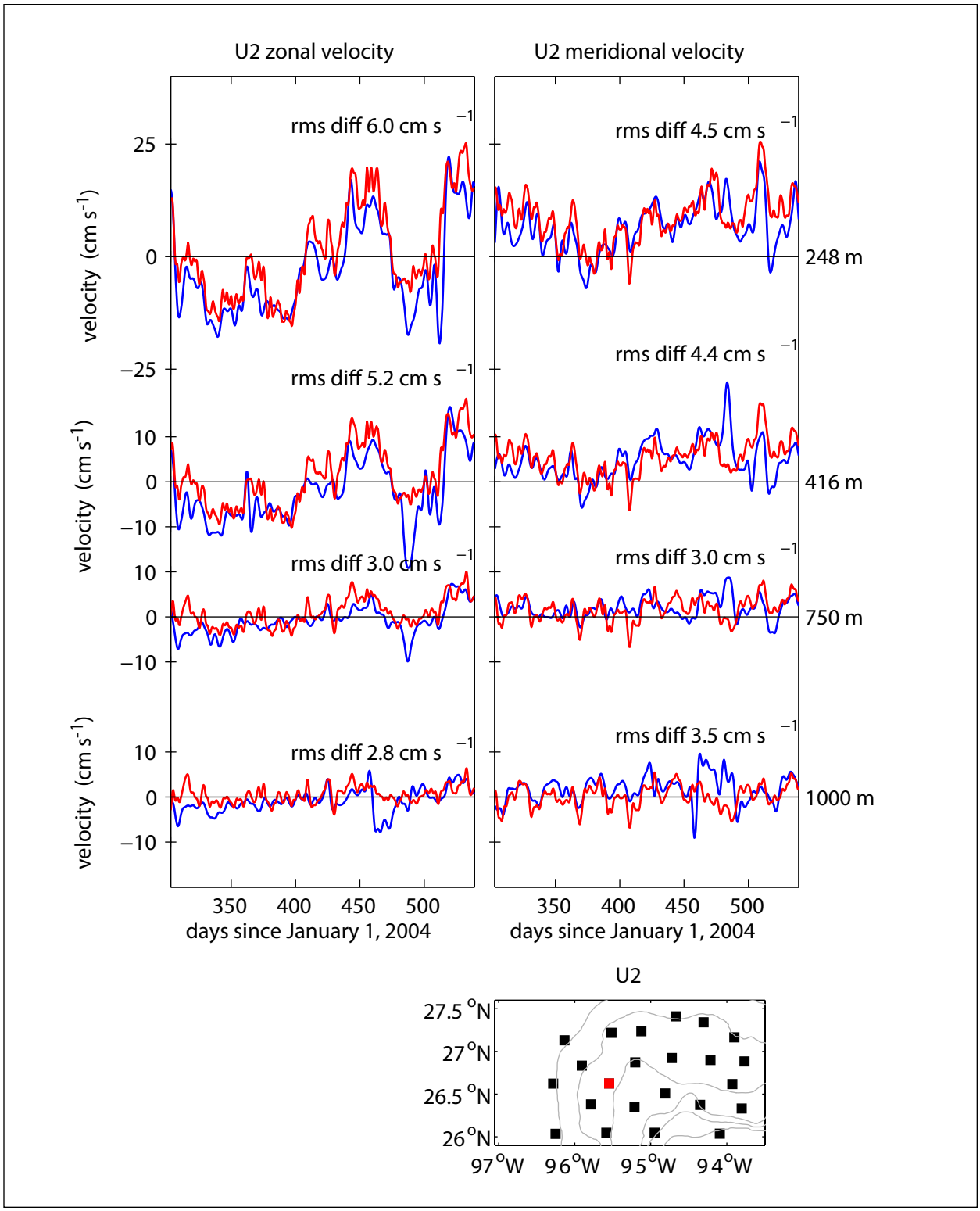

Figure 2-6. Comparison between the U2 mooring (blue) and PIES-derived (red) zonal (left) and meridional (right) velocities. The nominal depth and rms difference between PIES and the U2 mooring are noted to the right of each series. The bottom panel shows the location of the PIES (black) and pseudo-IES (black) and the U2 mooring (red). Bathymetry contoured every 500-m depth.

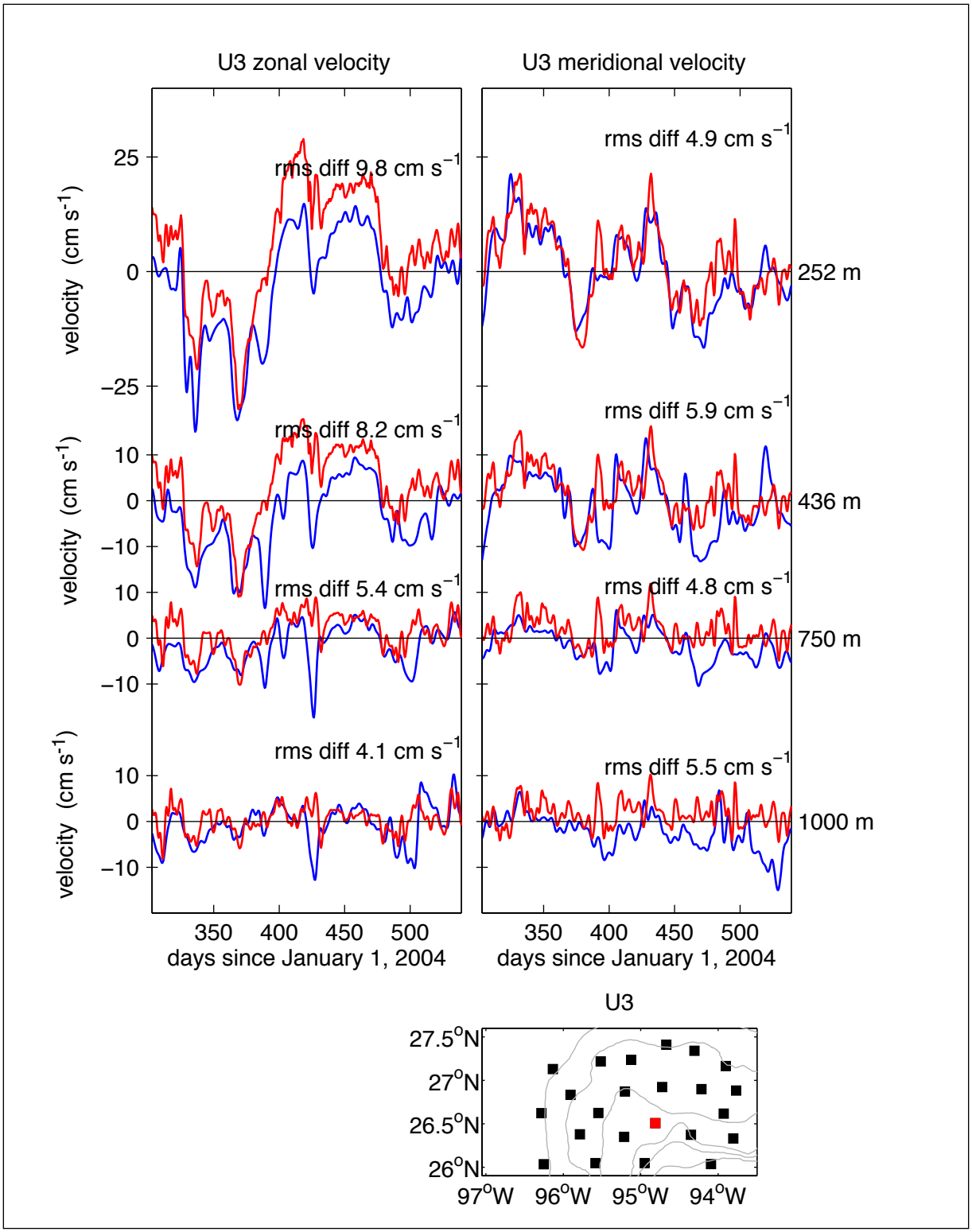

Figure 2-7. Comparison between the U3 mooring (blue) and PIES-derived (red) zonal (left) and meridional (right) velocities. The nominal depth and rms difference between PIES and the U3 mooring are noted to the right of each series.The bottom panel shows the location of the PIES (black) and pseudo-IES (black) and the U3 mooring (red). Bathymetry contoured every 500-m depth.

Within Volume II of this report is a detailed discussion of processing methods for satellite remotely sensed data. For details of that procedure the reader is referenced to that volume. There were three types of remotely sensed data used in this study: altimetry, sea-surface temperature and ocean color. An extensive amount of work went into the processing methodologies along with checking and verification of the procedures. It is of note that placement of PIES was in part determined to provide information on SSH along satellite track lines. The combined pressure and hydrographic information that is measured or derived from the PIES instruments provides a valuable comparison data set for the satellite-based SSH estimates. Results of some of such comparisons indicate that higher satellite repeat cycles produce better correlations with PIES SSHs.

An example presentation of SSH information is shown in Figure 2-8. In this and similar figures, warmer tones (yellow to red) are increasing height above a nominal zero while cooler tones (green through blue) are for decreasing height below a nominal zero surface. In viewing these color-coded images, the warm-centered features generally have an anticyclonic (clockwise) sense of rotation and cooler core features can be expected to have cyclonic (counter clockwise) sense of rotation.

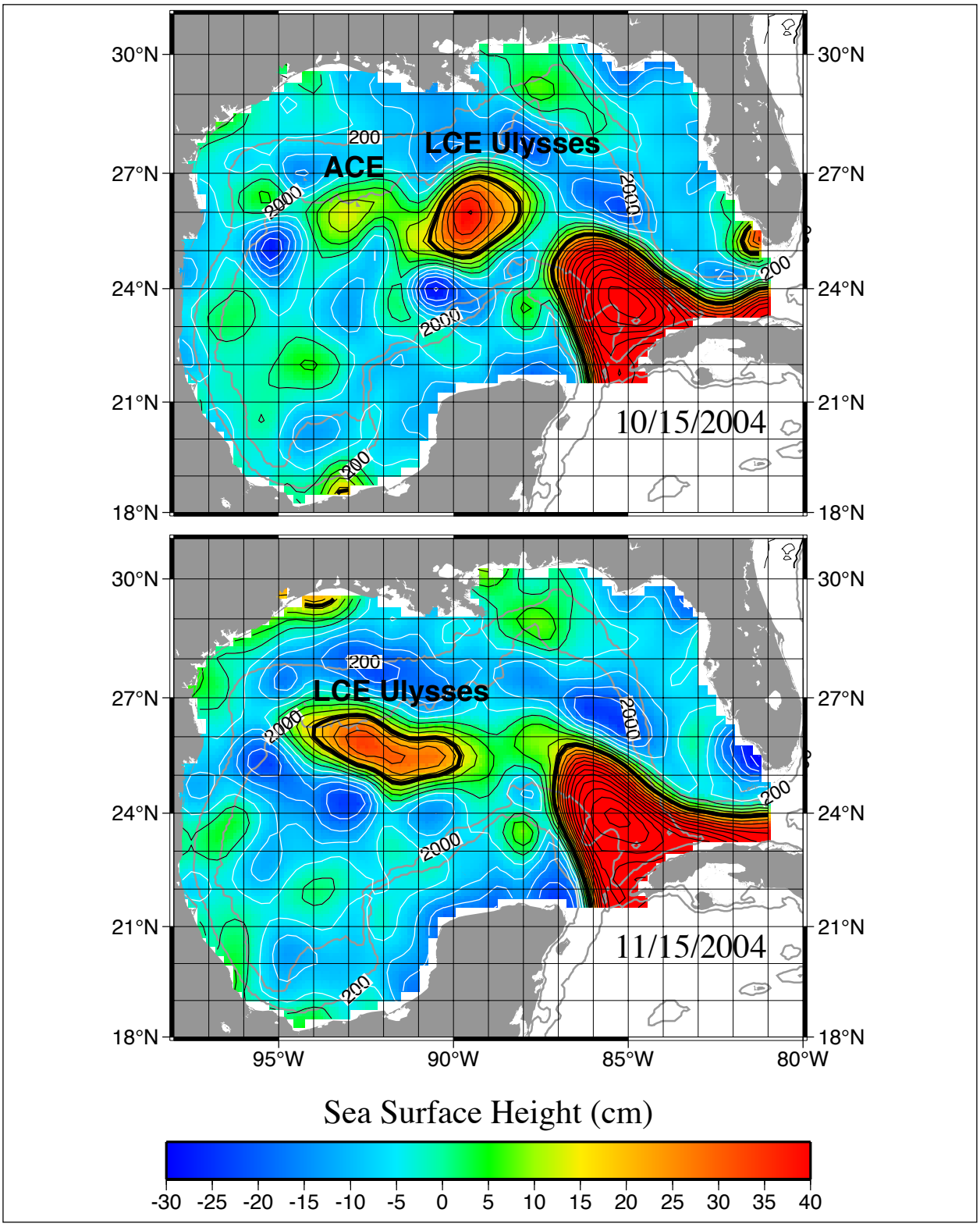

Figure 2-8. SSH maps of LCE Ulysses before (upper panel) and after (lower panel) merging with an anticyclonic eddy in the western GOM.

CHAPTER 3 UPPER-OCEAN CIRCULATION

The Loop Current (LC) and its associated mesoscale eddy field dominate the upper-ocean circulation in much of the deepwater of the GOM as a result of the strength of the current and their limited area of the semi-enclosed GOM basin. Aperiodically, the LC intrudes northward and westward into the GOM to form a loop of clockwise-flowing current extending from the Yucatan Channel into the deep GOM basin and out through the Florida Straits. At irregular intervals, ranging from a few months to as long as 18 months (Sturges and Leben, 2000; Leben, 2005), the looping segment of the LC closes to form a ring of current that completely detaches and separates from the LC to transport the contained water westward through the GOM as an anticyclonic oceanic vortex. This ring of current is commonly referred to as a Loop Current eddy (LCE). Like the majority of the deepwater GOM, the western GOM is strongly influenced by the LC. This influence, however, is not usually by direct intrusion of the current into the region. Rather it is more typically indirect, resulting primarily from the westward advection of LCEs (Elliot, 1982).

Using processed and integrated multi-satellite altimetry, it is possible to estimate the location and geometry of the LC. LCEs that have separated from the LC proper can also be defined with altimetry. Based on considerable prior work, it has been determined that the location of the 17-cm contour can be used as a surrogate for the boundary of the LC and for newly separated LCEs. Following the 17-cm contour that enters the GOM via the Yucatan Channel, metrics of the LC can be estimated. Among others, these metrics include the area of the LC, and the length of the LC boundary. Consideration of the LC area as a function of time, it is possible to identify when LCEs separate from the LC by evaluating the area time series for rapid reductions (Figure 3-1). When a separation occurs, the 17-cm contour shortens as the eddy removes some of the extended LC water mass. Following separation, the boundary of the LCE can also then be estimated by the closed 17-cm contour. Using similar criteria and automated processing of altimetry data, the movement of LCEs can be identified, as can the eddy center and areal extent. Because the maximum height of the eddy center decreases as the LCE moves across the GOM, a decreasing center height helps establish the location of the eddy center. This tracking procedure can continue into the western Gulf until the eddy elevation cannot be distinguished from the background SSHs. Using the altimetry data, 20 LCE separations have been identified over the 13.5-year interval (January 1993 – June 30, 2006) during which processed SSH data are available. A listing of these LCEs and associated information is given in Table 3-1.

In conjuction with the information in Table 3-1, computer processing of the GOM altimetry field supports a reconstruction of the movement of the identified LCEs. A review of the altimetric record found that LCEs often merge and split. Merging occurs when LCEs coalesce with nearby anticyclones or existing LCEs (Lewis and Kirwan, 1985; Kirwan et al.,1984; Berger et al., 1996). Splitting or cleaving (Biggs et al., 1996; Donohue et al., 2006) occurs when pieces of anticyclonic circulation of varying size split off from a LCE through the interaction of the eddy with peripheral cyclones. During this study when cleaving occurred, both parts of the original LCE were tracked so that their influence on the western GOM circulation could be better documented and understood. When merging occurred the combined eddy was tracked as one with documentation that merging had occurred.

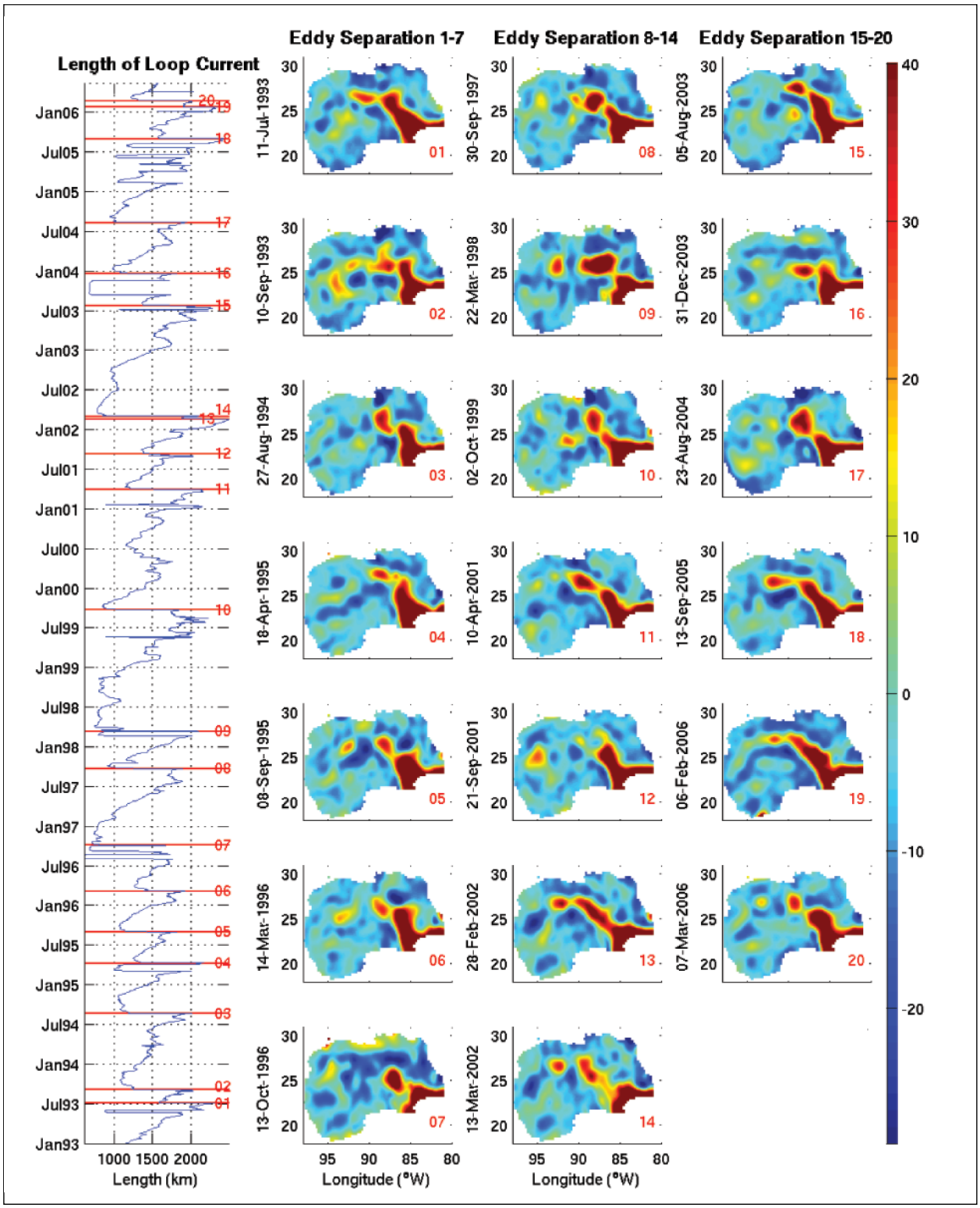

Figure 3-1. LCE separation events identified in the altimeter record. SSH maps on the separation dates are shown in the panels to the right (values above 40 cm and below -30 cm have been clipped). The LC length time series is overlaid with red lines corresponding to the separation dates.

Table 3-1

Loop Current eddy (LCE) separation events from the altimetric record: 1 Jan 1993 through 30 June 2006

LCE Number	Separation Date	Separation Period (months)	Industry Eddy Name	Area (km^2)	Eddy Maximum SSH (cm)
1	11 Jul 1993	11.5	Whopper	24,183	33
2	10 Sep 1993	2.0	Xtra	38,481	39
3	27 Aug 1994	11.5	Yucatan	43,022	39
4	18 Apr 1995	7.5	Zapp	21,337	36
5	8 Sep 1995	4.5	Aggie	24,899	36
6	14 Mar 1996	6	Biloxi	24,912	32
7	13 Oct 1996	7	Creole	49,644	69
8	30 Sep 1997	11.5	El Dorado	49,229	56
9	22 Mar 1998	5.5	Fourchon	89,143	72
10	2 Oct 1999	18.5	Juggernaut	40,325	39
11	10 Apr 2001	18.5	Millennium	45,705	44
12	21 Sep 2001	5.5	Odessa/Nansen	?	12
13	28 Feb 2002	5.5	Pelagic	22,119	41
14	13 Mar 2002	0.5	Quick	49,936	41
15	5 Aug 2003	17	Sargassum	25,302	49
16	31 Dec 2003	5	Titanic	33,278	43
17	23 Aug 2004	8	Ulysses	68,633	42
18	13 Sep 2005	12.5	Vortex	29,541	38
19	6 Feb 2006	5	Walker	11,366	29
20	7 Mar 2006	1	Xtreme	22,111	37

Tracking of the movement of the eddy center allows estimation of the various paths followed by LCEs as they move from the eastern basin to the western basin and eventually reaching the western GOM continental slope. Examples of these analyses are shown in Figure 3-2. Such "spaghetti diagrams" are visually difficult to interpret. By using several averaging techniques, mean paths can be computed and identified. The mean path in conjunction with the standard deviations of the path location provides a more "consumable" representation of the movement of LCEs from separation to eventual western GOM dissipation (Figure 3-3 through 3-5). As shown in these figures, the mean paths goes south of the present study area, intercepting the western slope in the vicinity of 23.5 – 24°N. Of the LCEs tracked using 13.6 years of altimetry, only three had the eddy centers that were at some point within the present study area (Figure 3-6). These three LCEs did not occur during the present study interval.

The key conclusion of the evaluation of the most energetic anticyclonic and cyclonic events in the historical record is that all were associated with LCEs. Thus, the LC is a dominant source of eddy energy even as far away as the continental slope in the extreme northwestern corner of the GOM. The LC influence is indirect and caused by the propagation of LCEs into the western GOM, and in some cases propagation into the study region. The LC may not only influence the intensity of the eddy field, but also the number of cyclonic eddies. The kinematic analysis of surface current and lagrangian drifter (SCULP) tracks by Hamilton (2007) suggests a possible link between the LC and the number of cyclonic eddies along the northern continental slope through the influence of propagating LCEs. Thus, there is strong observational evidence that eddy activity in the NW Gulf study region is related to the LC and LCE shedding cycle.

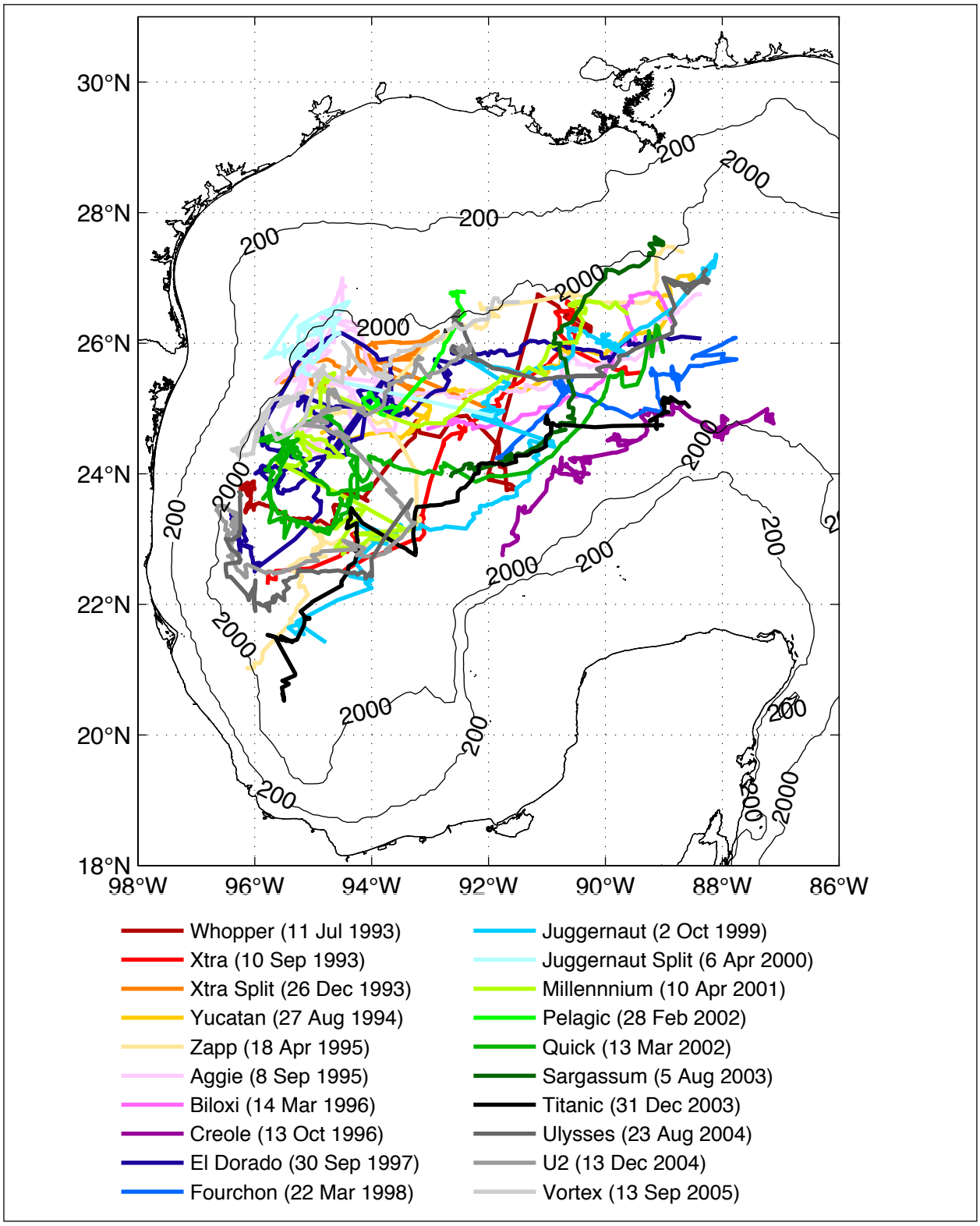

Figure 3-2. LCE center paths through the western GOM taken by the 17 LCEs and the three "split" eddies tracked using satellite altimetry.

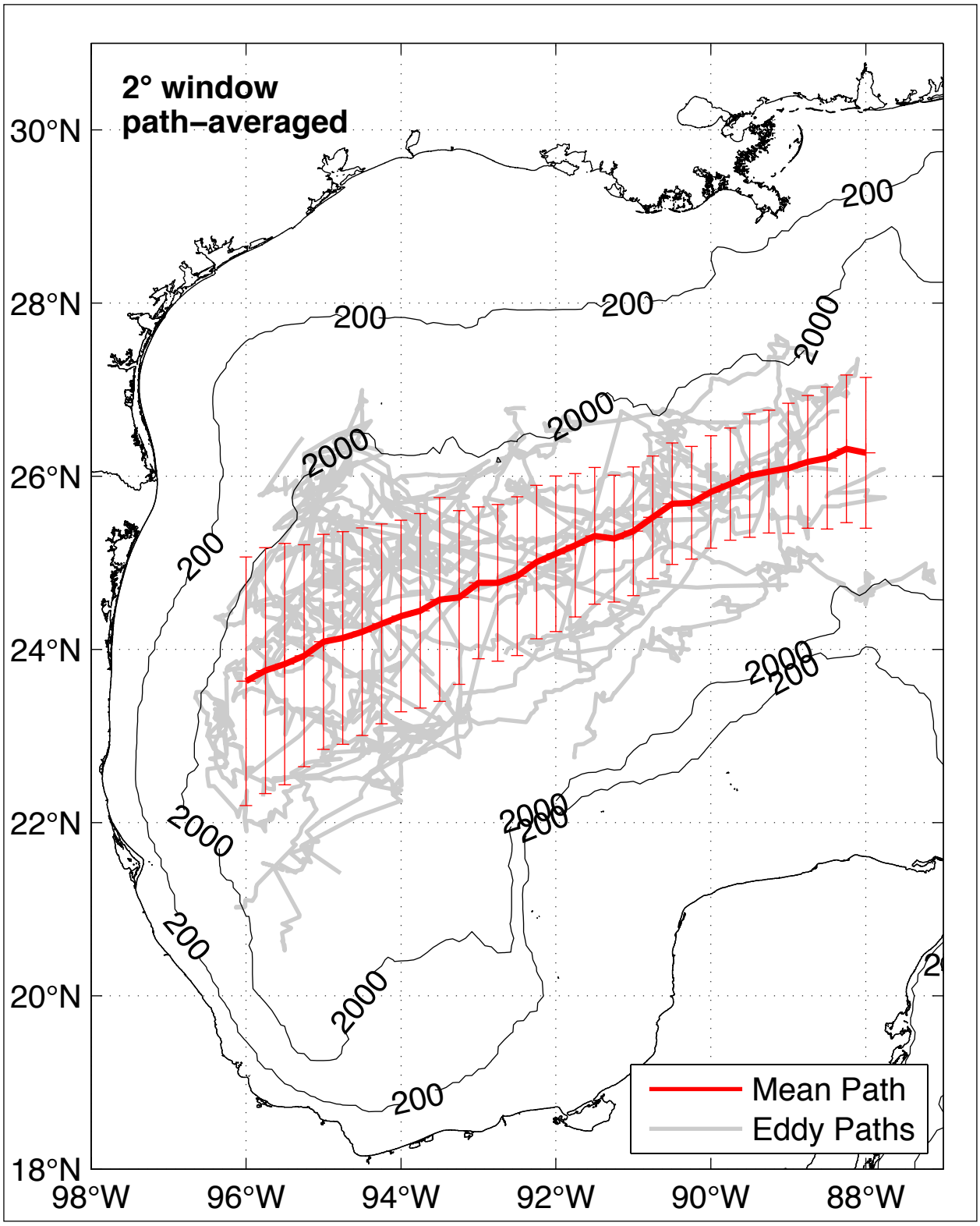

Figure 3-3. The 2° path-averaged mean path overlaid on altimeter-tracked LCE center paths.

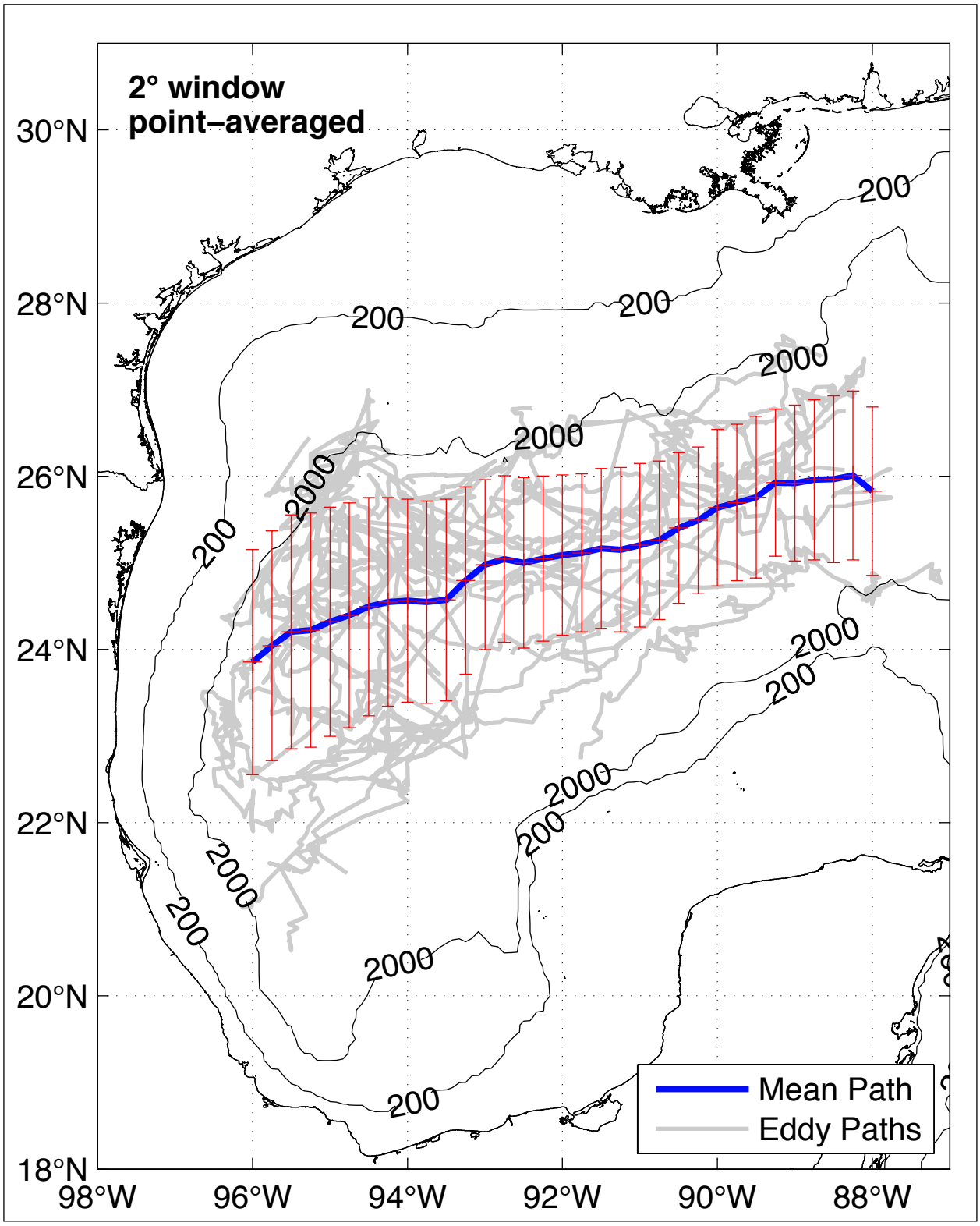

Figure 3-4. The 2° point-averaged mean path overlaid on altimeter-tracked LCE center paths.

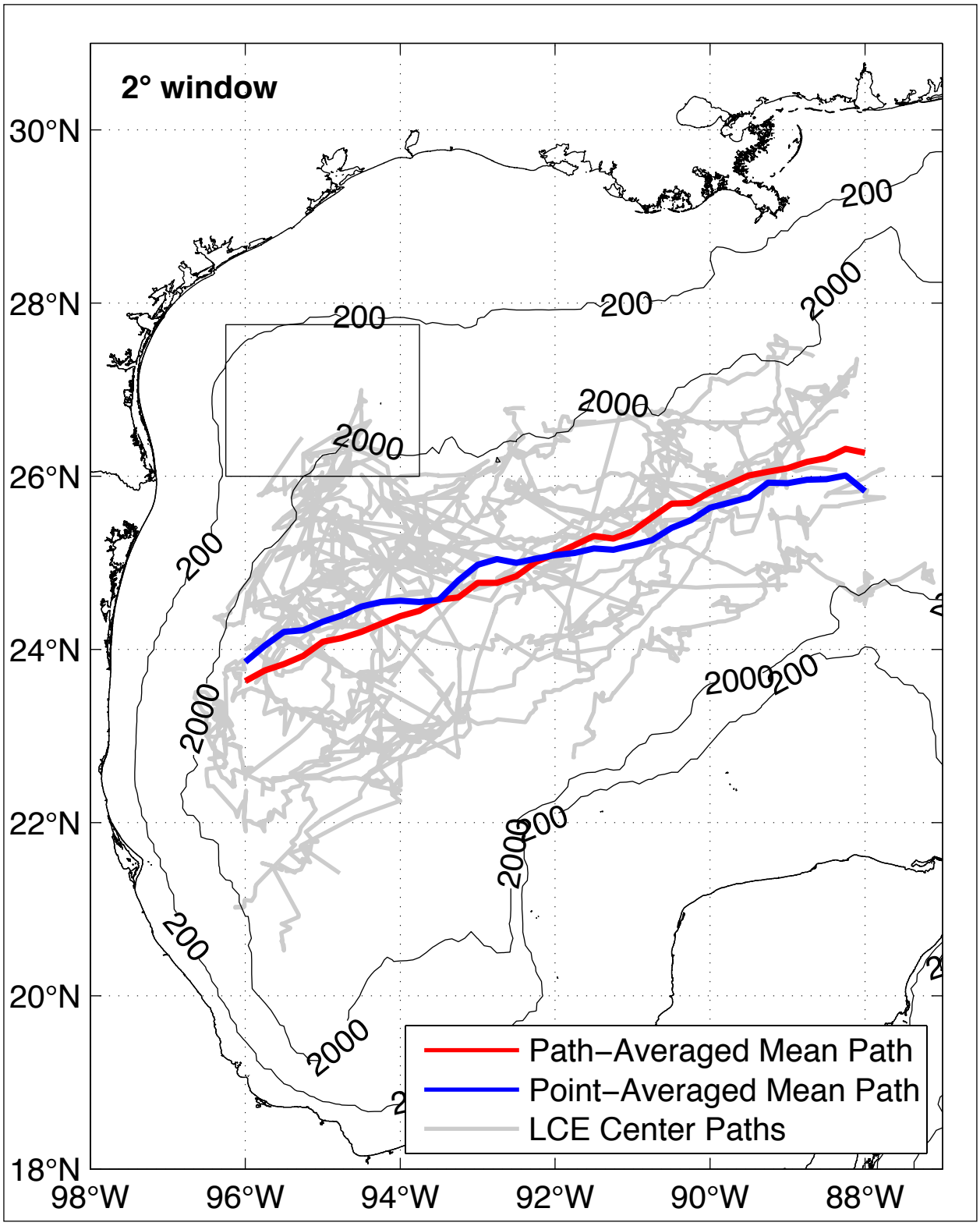

Figure 3-5. Path-averaged and point-averaged mean paths (2° averaging window) are shown overlaid on altimeter-tracked LCE center paths. Box identifies NW Gulf study region.

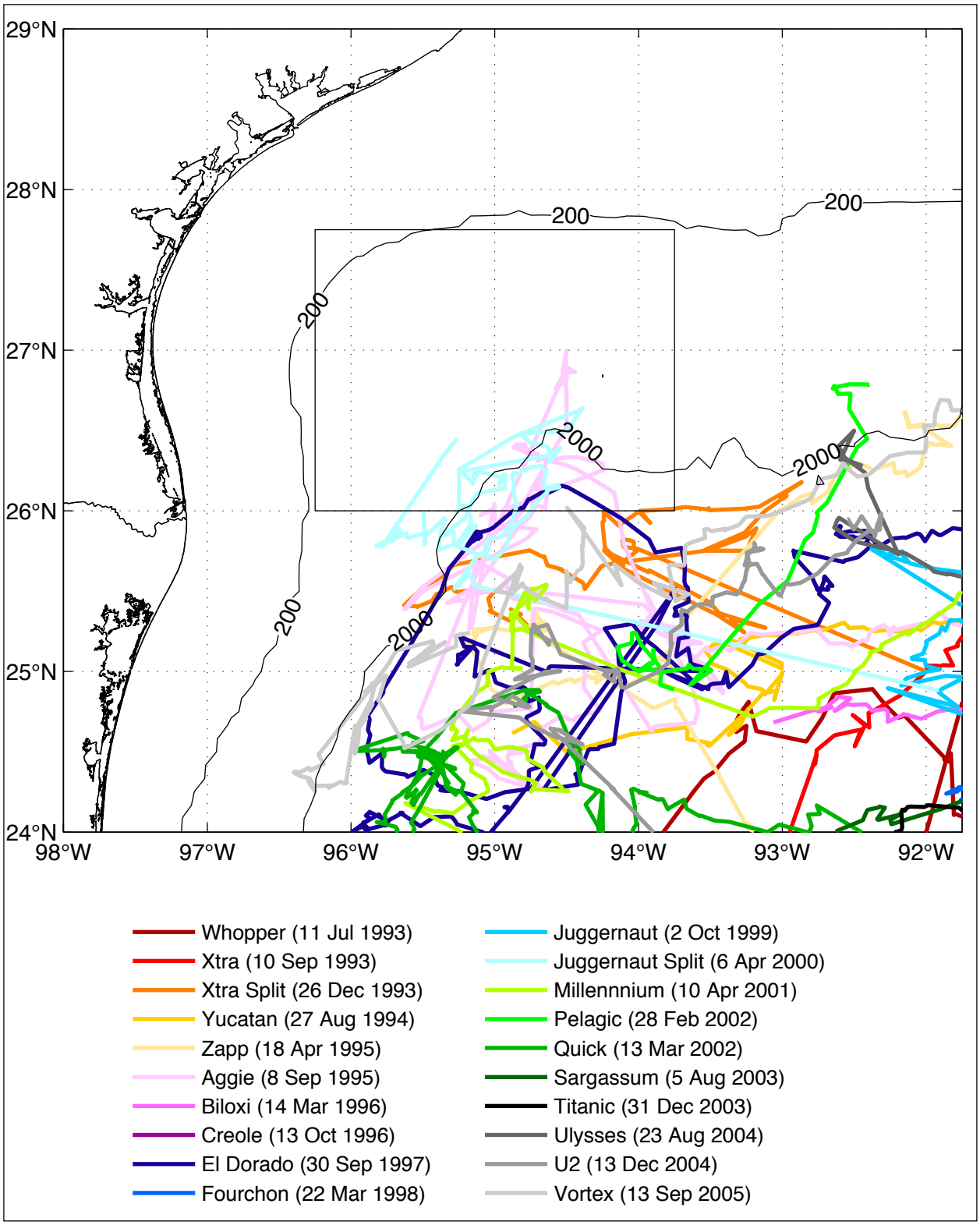

Figure 3-6. Altimeter-tracked LCE centers in the northwestern GOM. Box identifies NW Gulf study region. Centers of four LCEs were tracked into the study region: Xtra Split, Aggie, Juggernaut Split, and El Dorado.

LCEs during the NW Gulf Study

During this overall study in the western GOM (American and Mexican Sectors that extended between March 2004 through October 2005) three LCEs affected the upper-ocean circulation. These were, in chronological order, Titanic, Ulysses and Vortex (Table 3-1).

Eddy Titanic followed a more southerly path across the GOM staying well south of the study area. Once in the western GOM and interacting with the western continental slope, Titanic rapidly dissipated and after one month became indistinguishable from background SSH. While this LCE appeared to undergo a splitting event with each portion eventually moving separately, there was no evidence that the induced circulation associated with Titanic impacted the American sector of the NW GOM.

LCE Ulysses (life span 237 days with 125 being after splitting into two smaller eddies) had an initial area of 68,633 km^2 with a maximum SSH of 42 cm. In terms of area, Ulysses was the second largest eddy documented in the almost 14-year altimetry record. In its life span, Ulysses both merged with another anticyclone in the western GOM and later split/cleaved into two definable anticyclones. If the subsequent splitting was associated with the prior merger is not known. U2, as the more northern of the divided anticyclone was named, moved into portions of the present program field measurement array. The splitting process took about two months and coincided with Ulysses colliding with a strong cyclonic eddy located against the continental slope centered at 25°N. This history of eddy-eddy (anticyclone-cyclone) interaction and eddy-bathymetry interaction was a nonlinear process that substantially reconfigured the eddy field in the NW GOM. A comparison of altimetry with measured temperatures and salinities, such as the presence of SUW, supported the presence of U2 within the study area. U2 was the dominant upper-ocean event affecting the study region during these field observations. This influence was intermittent in the sense that as the eddy and possible daughter eddies migrated in the dissipation process, they moved into and out of the fixed instrumented study area. Eventually, U2 merged with the other portion of the Ulysses LCE. During the tenure of Ulysses/U2 in the western GOM, a complex sequence of smaller-scale cyclones and anticyclones occurred in the study area. These moved and interacted with one another and were significant factors affecting the observed upper-layer circulation patterns within the study area.

Eddy Vortex had four partial “separation events” prior to finally separating from the LC and traveling west southwest. On reaching the western continental slope, it interacted with a slope cyclone resident in the area south of the Mexican Sector moorings. As a result of interacting with both bathymetry and the cyclone, Vortex’s central elevation diminished by half in one month, reflecting a rapid weakening of this feature.

The presence of LCEs also affected the destructive hurricane seasons in 2004 and 2005. Because movement of hurricane winds over the ocean surface tends to mix waters in the surface layer, it tends to cool the water surface. However, with LCEs with their large reservoir of warm water, cooling is diminished and the underlying water surface remains relatively warm, providing the continuing energy source that supports maintenance or growth of hurricane intensity. An example of the movement of the center of Hurricanes Katrina and Rita relative to the underlying warm water “pools” associated with the LC and LCE is given in Figure 3-7 and 3-8.

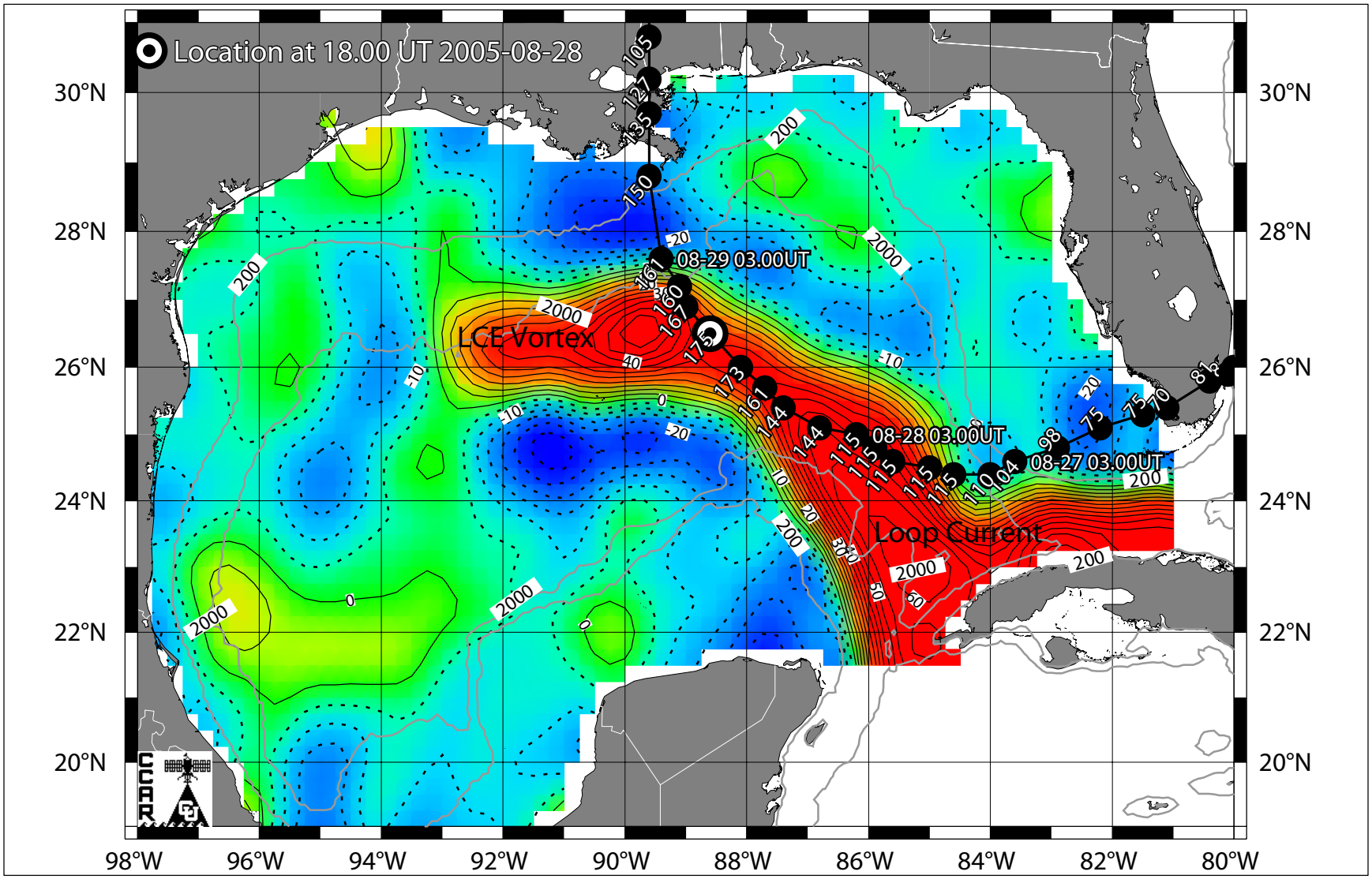

Figure 3-7. Overlay of Hurricane Katrina track and maximum sustained wind speeds (mph) on the 28 Aug 2005 SSH map.

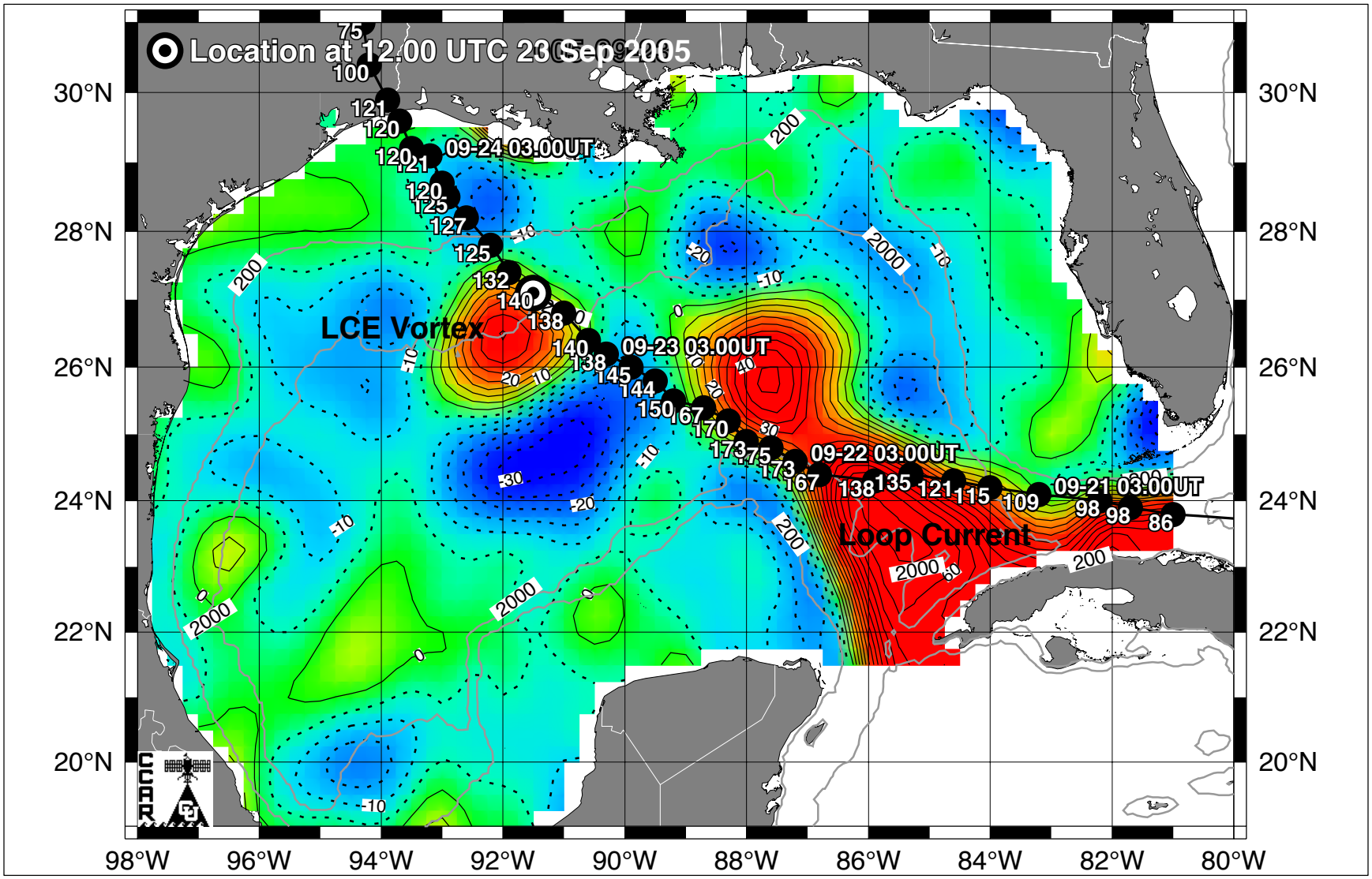

Figure 3-8. Overlay of Hurricane Rita track and maximum sustained wind speeds (mph) on the 23 Sep 2005 SSH map.

During this study, various combinations of remotely sensed and in-situ observations were used to develop a description of a complex series of primarily smaller-scale cyclones that were present in the study area and that interacted with one another, with anticyclones and the adjacent shelf waters. For a description of this complex sequence of features and interactions, the reader is referred to Section 3.3.4 of the Technical Report.

Basic Statistics

Developing statistical characterizations provides a different perspective as compared to the sequence of events described in the prior section. Comparison of statistics computed for the full American Sector deployment and the shorter interval that was concurrent with observations in the Mexican Sector are qualitatively the same. In the mean, the temperature field shows a warm eddy on the NW GOM slope, flanked by cold features to the northwest and northeast (Figure 3-9a) The currents were consistent with these features with anticyclonic flow over the NW slope and strong northward and offshore flow along the 2000-m isobath off the Mexican slope (Figure 3-9b). The mean current directions seem to have been in the same direction over the upper water column, with the largest magnitude currents occurring nearest the water surface. The highest velocity variance, which indicates that the eddy kinetic energy, was in the southwestern part of the American Sector array and at two moorings in the Mexican Sector. The variance decreased with depth representing a decrease in the amplitude of the fluctuating velocities with little apparent preference in the preferred direction of the fluctuations (i.e., orientation of the principal axes). This lack of preference indicates that the bathymetry did not tend to constrain the flow, except in the shallower water depth near the upper portion of the continental slope. Such a pattern would be consistent with a region where a variety of eddies moved through this upper layer. The average SSH and the associated mean surface currents are presented in Figure 3-10.

The profiles of velocity in the study region were such that at a single location, a single mode from Complex Empirical orthogonal function (CEOF) analysis could account for most (approximately 80% or more) of the variance of that profile. These analyses showed a pattern as described above, i.e., a decrease in magnitude with depth and a lack of preferred orientation except at the upper slope locations. Because of the large amount of variance accounted for by the single mode, it effectively incorporates the effects of many of the processes in the study area. Thus, use of the first mode to characterize these upper-layer patterns provides a convenient and concise method of examining patterns in the current profiles.

Computation of the kinetic energy spectra of first mode amplitudes showed that the largest energies were at the lowest frequency, a “red spectra”. This clearly suggests that the 15-month measurement interval was not of sufficient duration to resolve the complete frequency band of processes active in the area. While this information does not indicate the duration of observations that might be required, it is a clear indication that 15 months is too short to produce stable statistics for this eddy/event-dominated environment.

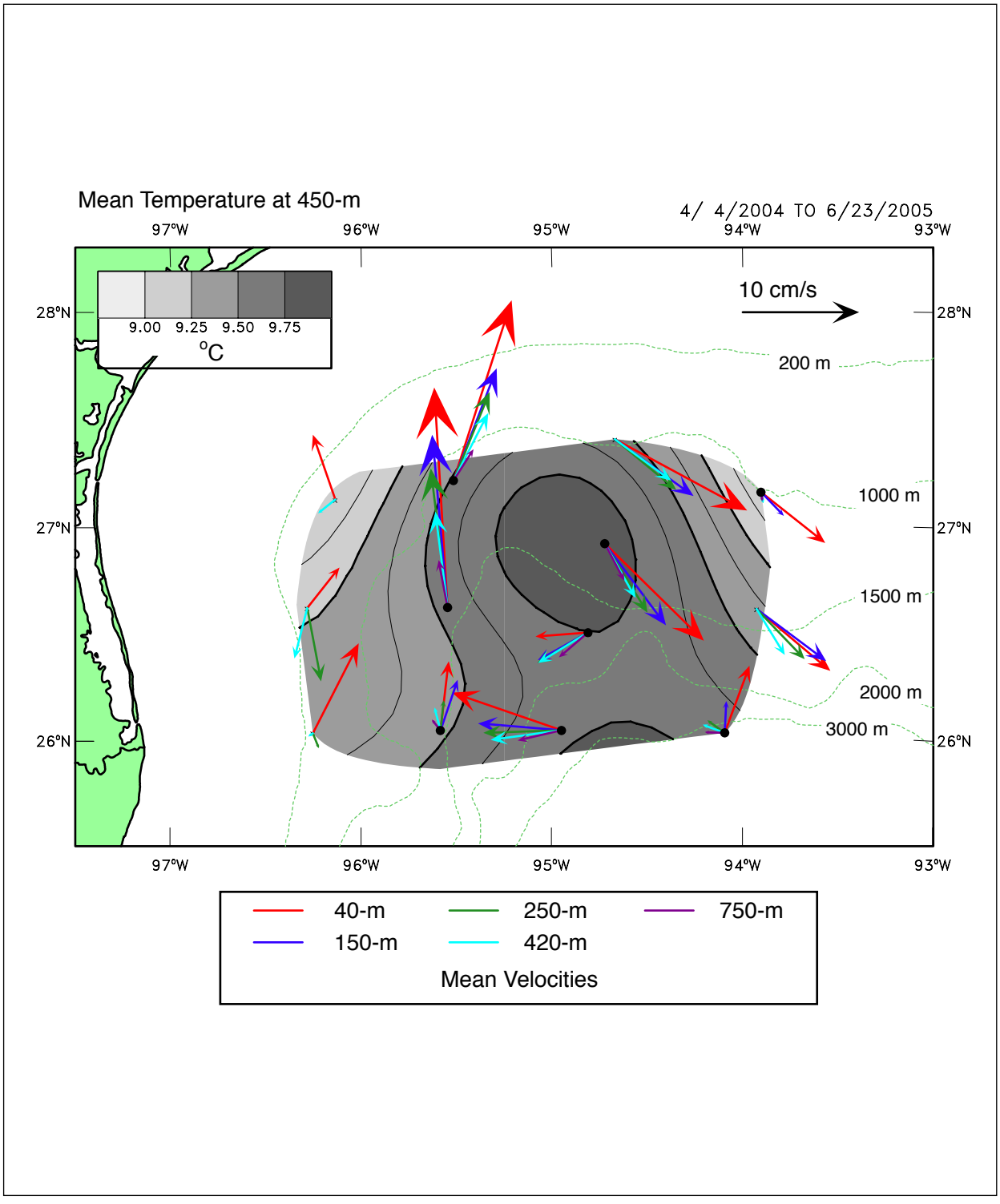

Figure 3-9a. Mean current vectors for the U.S. sector array, calculated from 40-HLP records, for the indicated interval and depths. The contoured mean 40-HLP temperature field at 450-m is also shown.

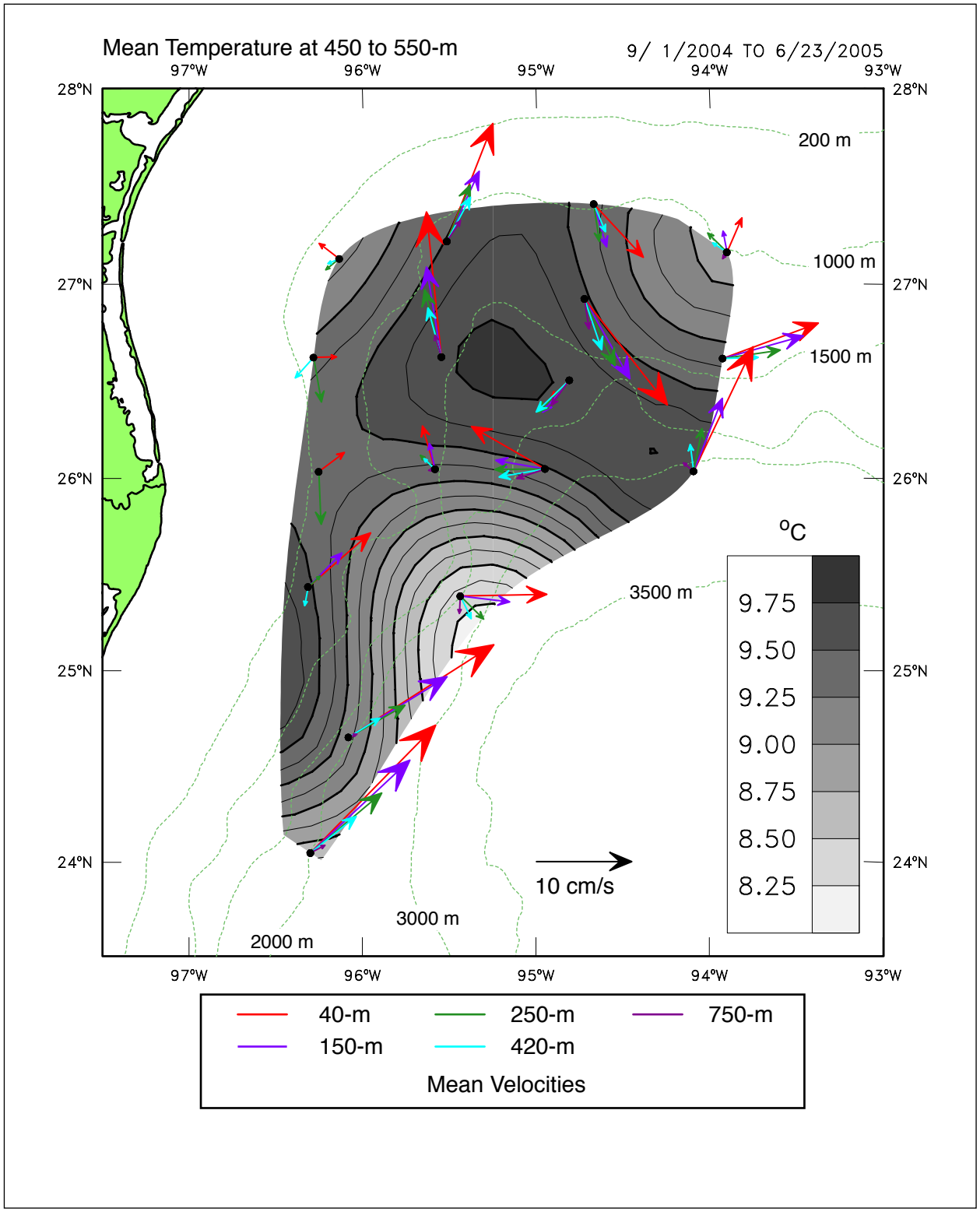

Figure 3-9b. Mean current vectors for the complete array, calculated from 40-HLP records, for the indicated common interval and depths. Note that the record at W1 is short relative to the common interval. The contoured mean 40-HLP temperature field at nominal depths of 450-m (in the north) to 550 m (in the south) is also shown.

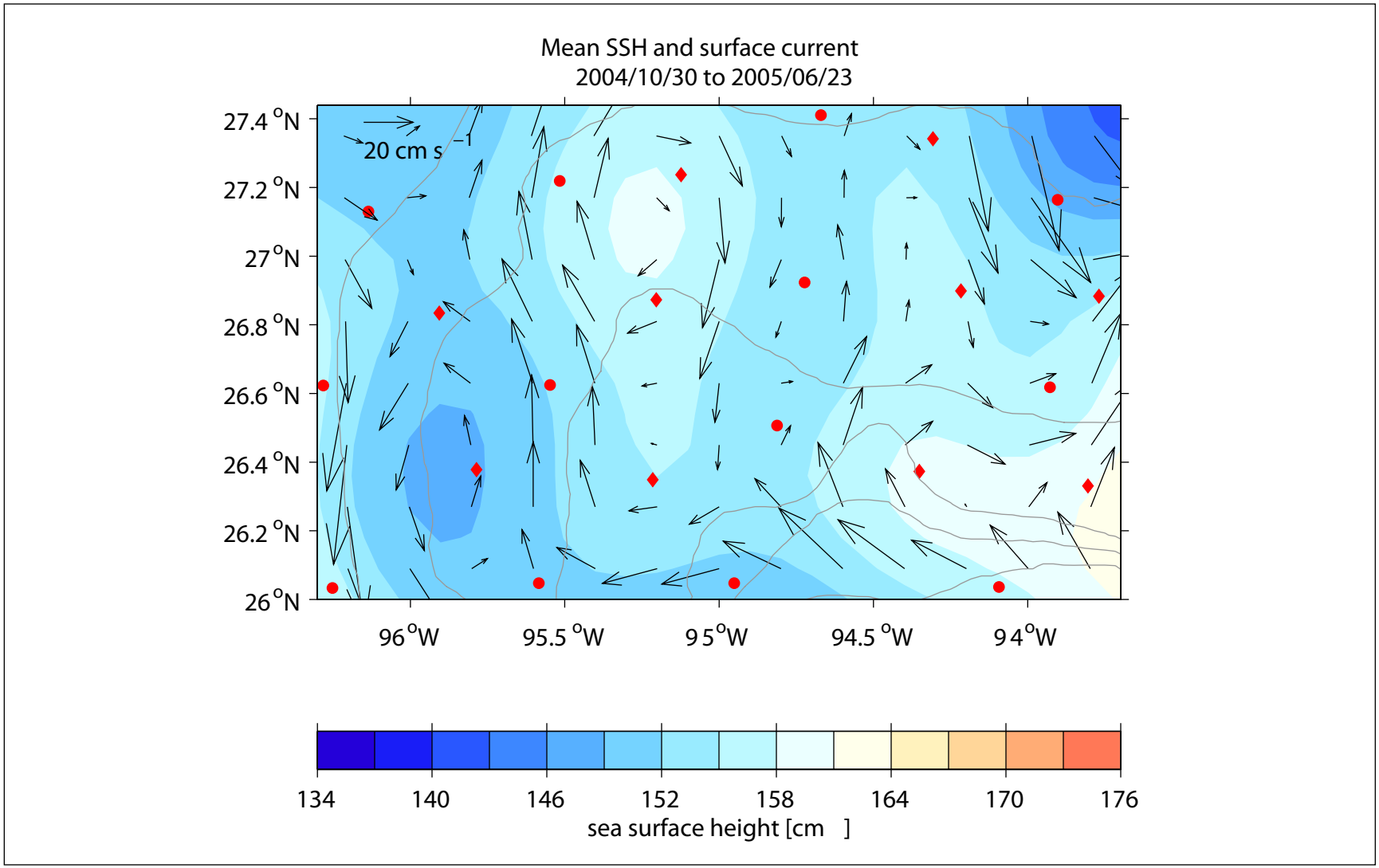

Figure 3-10. Time-average, mean sea-surface height (contours) and currents (black vectors) at the surface during the averaging interval from 30 October 2004 through 23 June 2005. SSH is contoured every 3.5 cm with low (high) values shown with blue (red) hues. Current vectors plotted at 20-km spacing. PIES sites indicated by diamonds, current meters denoted by circles. Vector key is shown in upper left corner. Bathymetry contoured every 500 m with gray lines.

When both measured currents and currents estimated from PIES observations, time-averaged currents for the coincident observation interval showed the mean upper-layer current was mainly anticyclonic and weak with mean speeds typically less than 20 $cm \cdot s^{-1}$ (Figures 3-9 and 3-10). These patterns of mean currents are consistent with those computed from moored instruments alone with some differences being attributed to the increased horizontal resolution resulting from the larger number of more-closely-spaced velocity estimates, and that the eight-month interval of coincident current meter and PIES observations did not sample the large anticyclonic eddy that affected the study area from June 2004 through October 2004. As would be expected, the largest eddy kinetic energy at or near the water surface was associated with LCEs or related cyclones. The primary LCE was U2 and eventually the combined influence of U2 and the other cleaved portion of this Ulysses.

Using currents and temperature information and a conservation of potential vorticity assumption, several examples were identified that illustrated the interaction of upper-layer eddy interaction with topography. The first example, in May 2004, was suggestive of the formation through PV conservation of cyclonic and anticyclonic slope flows resulting from flows that diverged from the isobaths. In May 2005, when both moored instruments and PIES were available, a similar set of features appear to have developed due to PV conservation. In this event-dominated environment, the occurrence of both these examples in May of different years was coincidental.

CHAPTER 4 DEEP CIRCULATION

Using deepwater observations taken in the mid- to late 1980s, Hamilton (1990) identified the likely presence of topographic Rossby Waves (TRWs) as dynamic processes that contributes to observed currents in the deep portion of the GOM. While the source of the TRWs was not clear, they had patterns that were consistent with expected behavior (e.g., wave velocity) of a TRW over the sloping bottom of the deep GOM. A significant element in identifying TRWs as an important contributor to deep current patterns is that the upper-layer and lower-layer current patterns were often decoupled. With the expansion of oil and gas industry interest in the deep portion of the GOM, substantial sets of new observations were made by industry and the MMS (e.g., Hamilton et. al., 2003). A key component of the role of TRWs in the lower layer, is that current profiles are strongly barotropic in the lower layer, i.e., relatively independent and constant with depth, and often bottom intensified so the strongest current magnitudes often occur close to the local bottom. Weakly sheared, deepwater current profiles have been a common pattern and recognized for a number of years. Using TRWs as a consistent cause of this pattern provided an explanatory process that could be extended to incorporate other features of these deepwater current patterns.

From an examination of available historical observations, it has become clear that lower water-column kinetic energy varies significantly by location. As an example, deep currents in the DeSoto Canyon were significantly different (and less energetic) than those measured just to the east in the vicinity of 90°W. Measurement at this later site at the base of the Sigsbee Escarpment documented currents as high as 90 $cm \cdot s^{-1}$ within 100 m of the bottom. These north-central GOM moorings were deployed for sufficient duration to provide important insights to the characteristics of TRWs and how they relate to limiting and steering environmental parameters such as local bottom slope. Use of numerical ray tracing points to the west side of the LC as a likely generation region of the shorter period, higher speed TRWs.

A more recent MMS-funded study (the Exploratory Study) found that the Sigsbee Escarpment had a profound effect on the transmission and reflection of TRWs, with the region above the top of the escarpment being relatively insulated from the effects of TRWs. Moreover, the escarpment and the slope at the escarpment base acted as a filter with short-period waves being trapped near the steep slope in the east while the western part of the region was dominated by much longer period (≈ 60 day) fluctuations. Motions with intermediate periods (between 10 and 60 days) appear to have been reflected back into deeper water with paths that suggest that not all these westward directed waves would reach the NW GOM.

Spectra, in variance preserving form, for lower-layer currents in the American Sector of the NW Gulf Study are presented in Figure 4-1. These show that, as might be expected from experience in the Exploratory Study, fluctuations above the escarpment were less energetic and had spectral peaks at different frequencies when compared to sites below the escarpment. There were other spatial variations in the current variances, but not as yet identified with a process-based explanation. Note that only two moorings in the American Sector, V3 and V4, were at or near the base of the escarpment. In this confined area a complex pattern of currents might be expected since the steep and incised escarpment could have a significant local effect on any

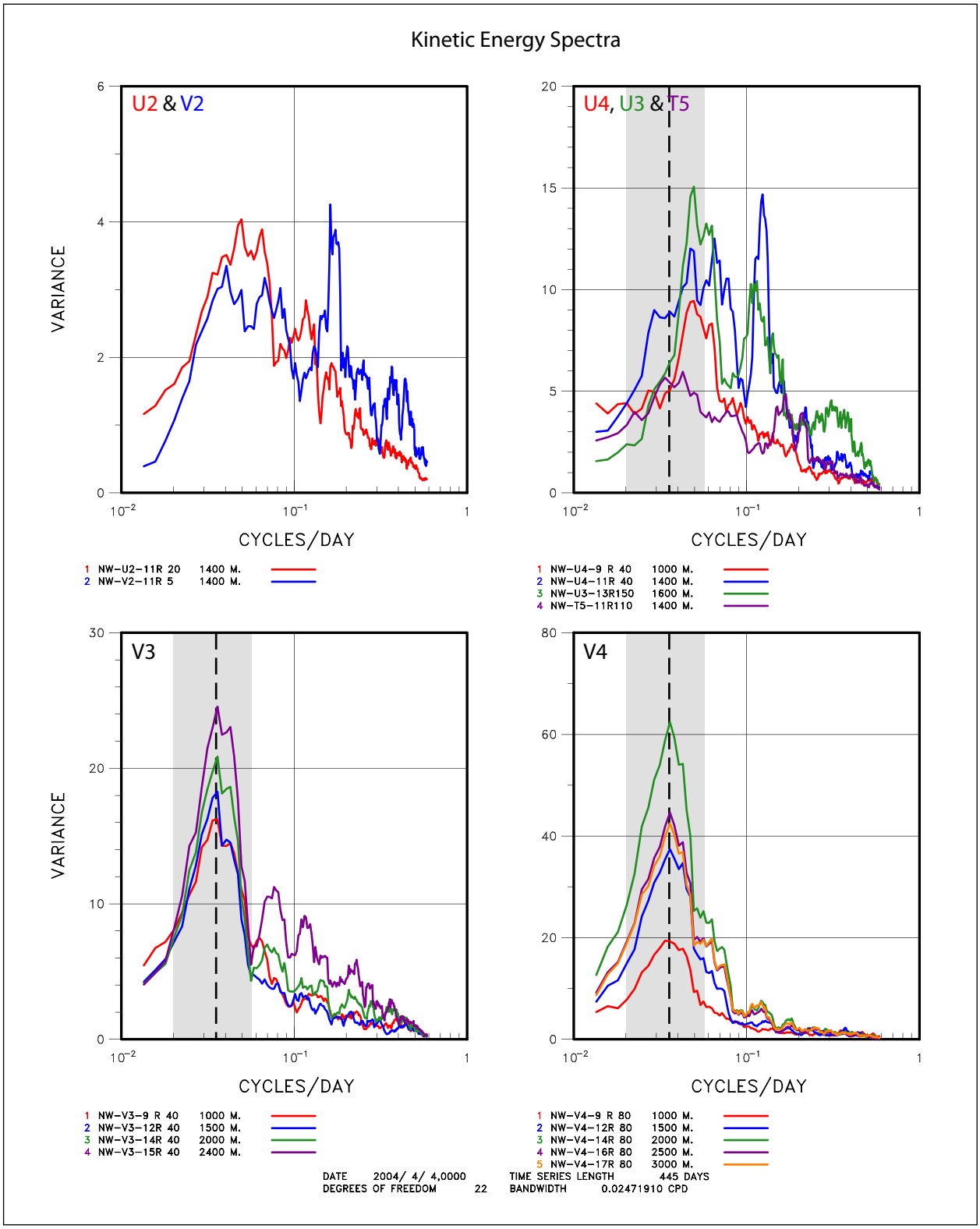

Figure 4-1. Kinetic energy spectra from the indicated 40-HLP records from lower-layer instruments on moorings in the U.S. sector. The dashed line and shading show the peak frequency and band of high energy at V3 and V4.

coherent wave motions in this region where bathymetry has a significant counterclockwise turn – the NW corner of the GOM.

Eddies vs. Waves

An initial discussion is provided of the potential relationship between what may be called a "wave" and what may be called an "eddy". Given the considerable discussion using these two descriptions, an effort is made to describe possible similarities and differences that may suggest the use of one description or the other. In the surface layer, items described as LCEs are recognizable as closed circulations that enclose and carry water with specific properties. In other surface features, things called eddies may not in fact transport mass, e.g., LC boundary features (often referred to as an eddy) are largely the configuration used to transmit momentum along the edge of the LC or on the boundary of a larger LCE.

In the discussion developed in Section 4.3 of Vol. II of this report, plane waves viewed in two dimensions contain fields of high and low pressure centers. Such a field of pressure centers can be generated by summing plane waves with wavenumber vectors crossing at an angle (Figure 4-2). The waves producing this situation may be originating from different location and/or reflecting off a boundary. The closed-core features in Figure 4-2 need not transport the core mass, but the core may propagate through the fluid. The argument is developed that whether a closed-core feature transports mass is determined by the ratio of the swirl velocity (U) to the translation velocity (C) of the feature such that if $U/C>1$, the features streamlines enclose a core whose mass and properties are carried with the feature. If $U/C<1$, the feature moves through the medium and does not carry a core. As a result of these factors, deep eddies can "appear in place' by constructive adding of various waves and subsequently "disappear" as the phases of the constituent waves change. If due to changes in eddy characteristics, a feature having at one time a ratio>1, subsequently has a ratio <1, it can tear the eddy-like feature apart. This also means that for a closed, transporting eddy to exist all the way from the eastern to western deep GOM, it should continuously have had a ratio >1 along the entire path.

The above discussion is relevant to consideration of moored current observations and those from PIES. Both data sources are measuring the same features, however, contoured stream function values often indicate the presence of rather ephemeral closed features. These features are in fact the result of cross wavenumbers from different locations for reflections. The moored observations and the PIES are both measuring motion due to TRWs.

TRWs

In our analysis of the TRWs, we concentrated our efforts on the three moorings that had more than two current measurements below the 1,000-m level, Moorings V3, V4 and W3. In the American Sector, for deep currents, the first EOF mode explained over 90% of the observed total variance. Fluctuations were fairly rectilinear with the major axis either parallel, or at a slight angle to, the general trend of the isobaths. Generally motions were in-phase through the lower water column with almost no change in direction of the major axis with depth. Although there were some slight variations in the expected patterns, these coherent current fluctuations through the lower water column are characteristic of TRWs and similar to those previously analyzed in

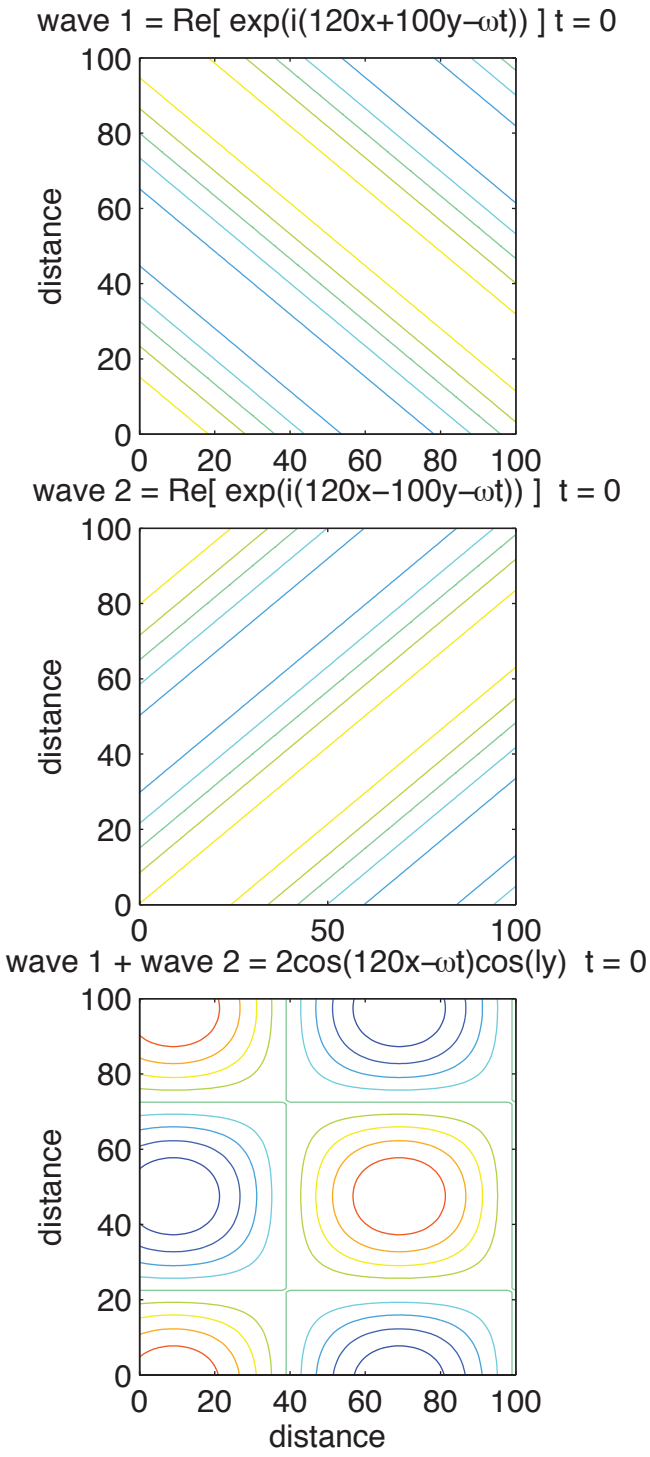

Figure 4-2. This idealized case is drawn from the sum of two waves, Re[exp(i(kx+ly-wt)) + exp(i(kx-ly-wt))] = 2 cos(kx-wt) cos(ly), which is a field of high and low pressure centers, modulated in two dimensions, propagating in the x direction. In this example, k=2 pi/100, and l=2 pi/120, and we view a snapshot at t=0. A localized wave group would comprise a bandwidth of k wavenumbers and l wavenumbers.

other regions of the GOM (Hamilton, 1990; Donohue et al., 2006). In the Mexican Sector, EOF modal analysis of currents at W3 differed somewhat from that to the north in that two modes were used to account for > 90% of the total variance in the 25-30-day period band. The lower frequency band centered on periods of 50-60 days and one mode accounted for 85% of the total variance in this band. The behavior of the major axis of these two frequency bands was consistant with prior observations in the northern GOM and as predicted by TRW theory.

Using ray tracing, a view of possible TRW ray paths for the period and wavelengths discussed in Vol. II of this report is shown in Figure 4-3. Importantly, the only reasonable path that connects to the eastern GOM is the down-slope 66-day period wave. As shown in Figure 4-3, the shorter 23-day period ray paths indicate that these motions were probably generated fairly locally and remained trapped in the corner region. Local sources may have been a result of surface eddies interacting with bottom over the lower slope.

Vertical Coupling

On an initial consideration, motion in the upper and lower layers appears to have been uncoupled in the NW GOM. An examination of animated data presentation revealed few patterns that appear to be linked between the layers. Even the array-averaged EKE of the upper and lower layers differed. Upper-layer EKE reflected primarily the propagation of LCEs and cyclones into and out of the array which did not correlate with more frequent strong lower-layer events. Deep eddy Kinetic energy (EKE) peaks were associated primarily with events along the northern and northwestern array boundary that may have been locally or remotely forced. To help evaluate possible vertical linkage, a ‘case study’ of vertical coupling was done that shows that the change in lower-layer potential vorticity was achieved primarily through the balance of vortex stretching and the production of relative vorticity. In this case study, an upper-layer cyclone entered the instrument array from the south and propagated north and westward. As the upper-layer cyclone advanced, the lower layer stretched and a deep cyclone developed.

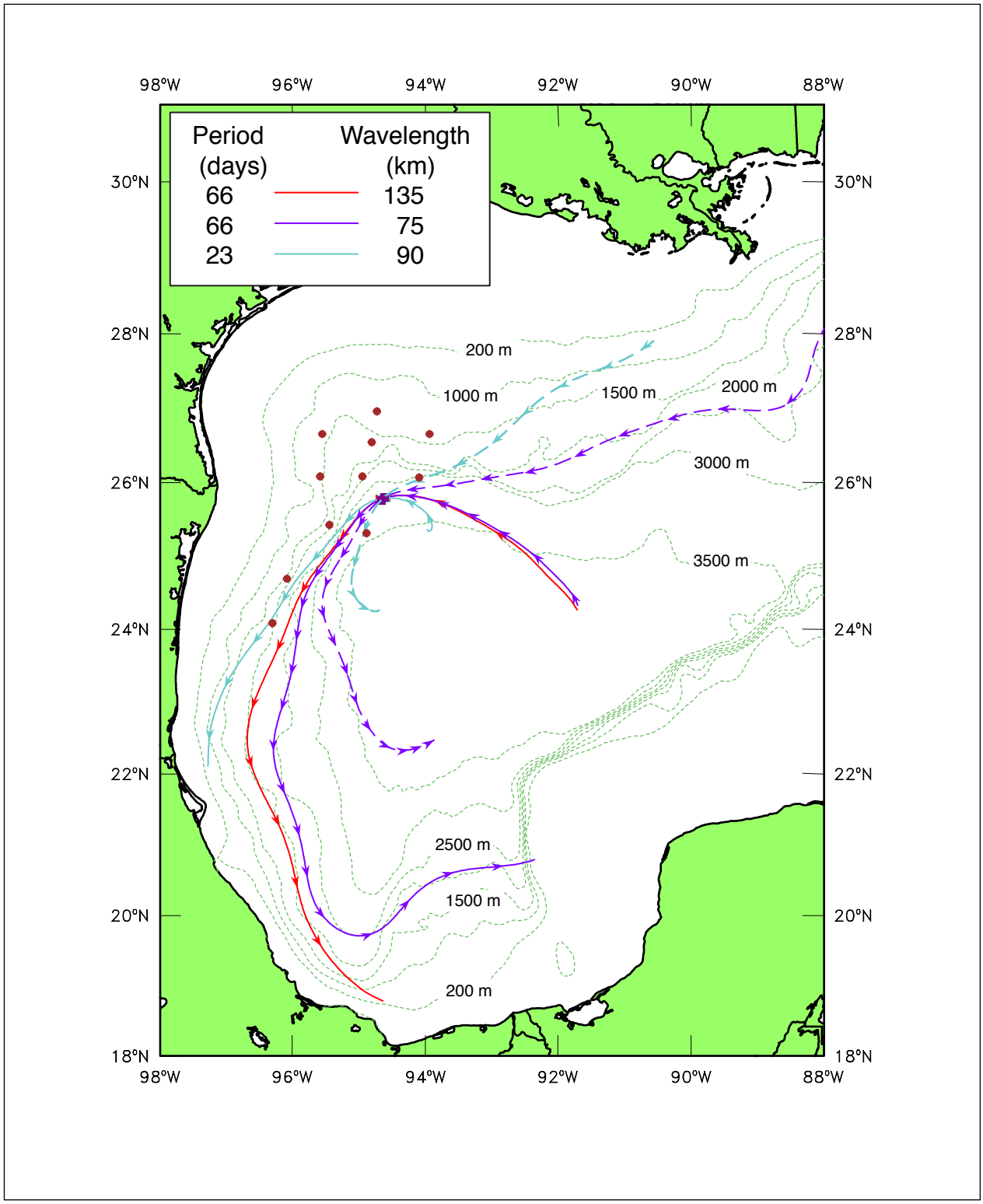

Figure 4-3. TRW ray traces for given periods and wavelengths. Arrow heads are at 5-day intervals, and solid and dashed paths are on- and off-slope propagating waves, respectively. Small solid circles are mooring locations.

CHAPTER 5 HIGH-FREQUENCY CURRENTS

In the GOM, inertial currents are characterized by clockwise rotary motions of current vectors that have periods determined by the value of the Coriolis parameter, f, which is a function of the latitude. In the northern GOM, this period is close to 26 hours that is very close to the diurnal tidal period. However, since the diurnal tidal currents in the deep GOM are small (a few $mm \cdot s^{-1}$), the current records can safely be evaluated without trying to remove these diurnal tidal currents from the observations.

Generation events for internal waves originating at the ocean surface are usually surface wind stress associated with a storm or a strong wind shift such as might be associated with passage of a cold front. Once initiated, the inertial-wave currents propagate vertically downward, although this produces an upward propagating phase. Since the group velocity is at a small downward angle to the horizontal, inertial currents measured at a given site may have been initiated at a location horizontally distant from the measurement site. An example of a vertically propagating inertial wave seen in this study is shown in Figure 5-1, where high-speed ($> 60\ cm \cdot s^{-1}$), approximately daily pulses propagated down through the upper 200-250 m of the water column over an interval of 12-15 days. Extrapolating these currents to the ocean surface, points to an abrupt wind shift (April 30) followed by strong ($\approx 15\ m \cdot s^{-1}$) northerlies that lasted about a day. As shown in Figure 5-1, the measured temperature at 350-m depth, which was below the region of energetic current fluctuations, showed large amplitude, approximately daily fluctuations from 6 to 11 May 2005. These temperature fluctuations with time imply a vertical motion of local isotherms, and hence a fairly large vertical velocity component at this level, and lesser magnitude vertical velocities deeper in the water column (450 m).

The effective value of the Coriolis parameter can be slightly modified by the relative vorticity where the inertial currents are occurring. The relative vorticity has both horizontal and vertical gradients caused by the mesoscale eddy, and the resulting variations in the effective vorticity can allow rapid propagation or trapping of inertial waves. In the example in Figure 5-1, mooring T3 was on the northern side of a slope anticyclone and the resulting relative vorticity was less than zero. This affect results in estimates that the effective vertical penetration of the inertial currents would be to a depth of approximately 250 m, as seen in Figure 5-1. Below approximately 300 m, horizontal motions were being converted to vertical motions as reflected by changes in the measured temperature time series in Figure 5-1.

While the surface forcing that excited the inertial waves described above was due to the frontal passage that moved rapidly over the entire instrument array field, the response to this forcing varied by location. Part of these variations resulted from the measurement location relative to the anticyclone mentioned previously. The resulting change in the value of the effective Coriolis parameter (modified by relative vorticity within the anticyclone) would help explain some of the spatial variations in response to the frontal passage forcing.

Hourly time series of PIES observations of elapsed acoustic travel time were also used to evaluate for near-inertial signals. In this approach, the inertial signal is contained in fluctuations of isotherms, more specifically the thermocline. Hence these will not reflect the currents

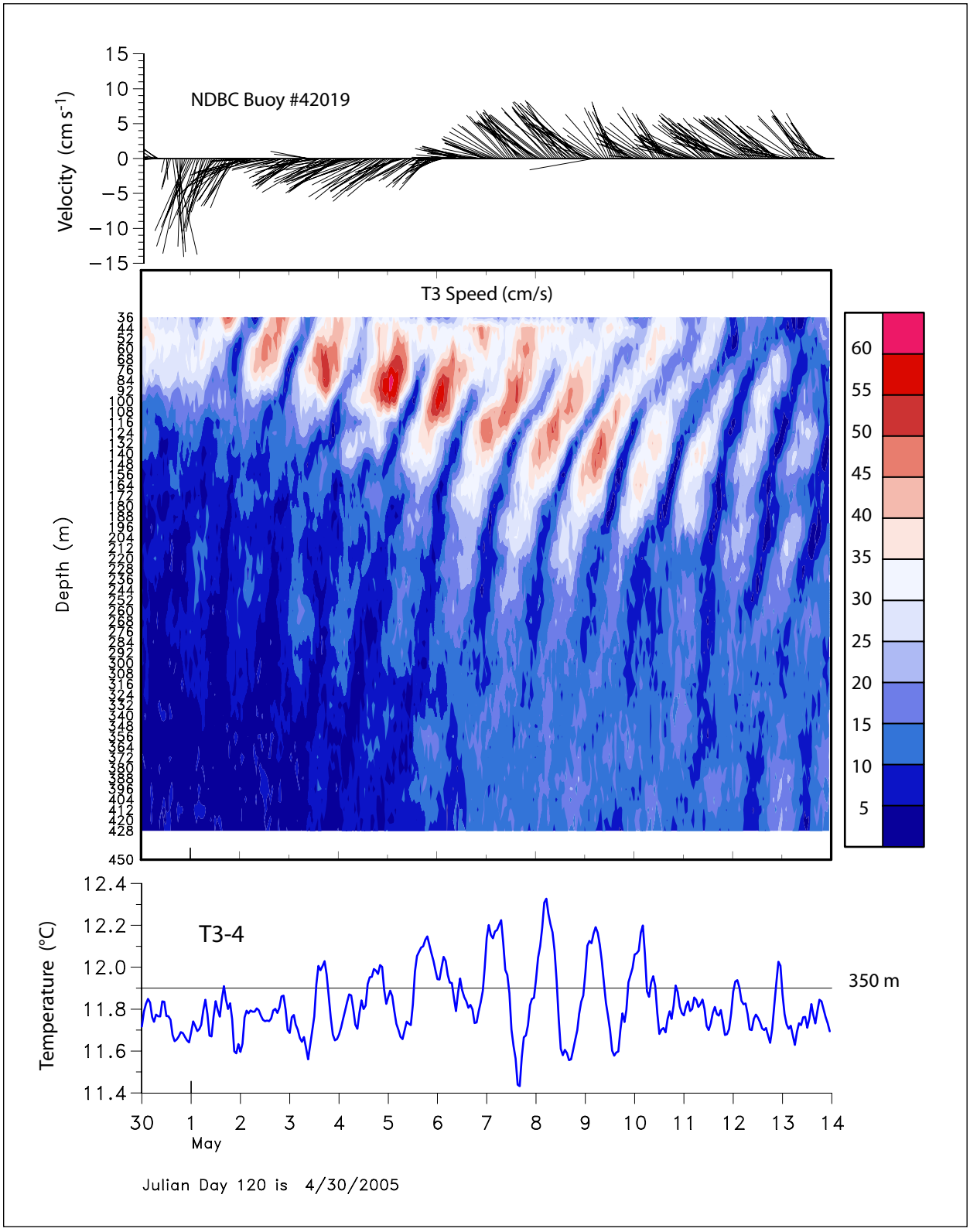

Figure 5-1. Unfiltered speed/depth observations from the upper-layer ADCP as measured at T3. Bottom panel shows the temperature record at 350 m, and the top panel the hourly wind vectors (up = North) from NDBC buoy 42019.

described above, but rather the larger vertical motions documented to be occurring below the region of stronger horizontal inertial currents.

These analyses of PIES records show bursts of energy in pulses that last 15-30 days (see Figure 5-2) that do not reveal a strong seasonal dependence, however, there was a tendency for the strongest events in each record (derived from data on each PIES) to occur in winter. When evaluated in terms of the position relative to mesoscale circulation features (e.g., LCEs) reveal a consistent pattern of enhanced motions. This low-mode inertial variance differs in magnitude and horizontal structure from that estimated from EOF evaluation of velocity records made by sensors on the moored arrays. The PIES-based and velocity-based observations of inertial waves are both affected by their location within mesoscale features such as LCEs.

Subsurface Jets

For this discussion, jets are defined as local or vertically isolated horizontal flows with maximum velocities of greater than 50 $cm \cdot s^{-1}$ (nominally one knot). Typically, these jets are identified as occurring at depths of 100 m to 300 m below the water surface as described by DiMarco et. al., (2004). Internal waves that may satisfy these general criteria are not the focus, rather interest is in relatively isolated features. During the NW Gulf Study, jets satisfying these criteria were documented three times with only two of the three instances occurring in deep water (>1,000 m). The third event was at a mooring in only 500 m of water depth.

One jet episode occurred at mooring T5 (Figure 1-2) located on the 1,500 m isobath. The currents were measured with an upward directed ADCP positioned at 450 m below the surface. A contour plot of the current speed (magnitude of the current vector) in the upper 428 m is shown in Figure 5-3. At three different times over a nominal six-day interval, speeds exceeded 70 $cm \cdot s^{-1}$ within the depth interval of 100 - 350 m. During this multi-day interval, these maximum speeds were localized in that lower speeds occurred both above and below the jets.

A possible explanation for this feature is suggested based on the evolving temperature structure at mooring T5. It appears that a cold cyclone and warm anticyclone were interacting at T5. Typically the jets occurred when isotherms at the depth of the jet episode were diverging, often as the result of the cyclone moving into the area and causing local cooling at the level of the jet.

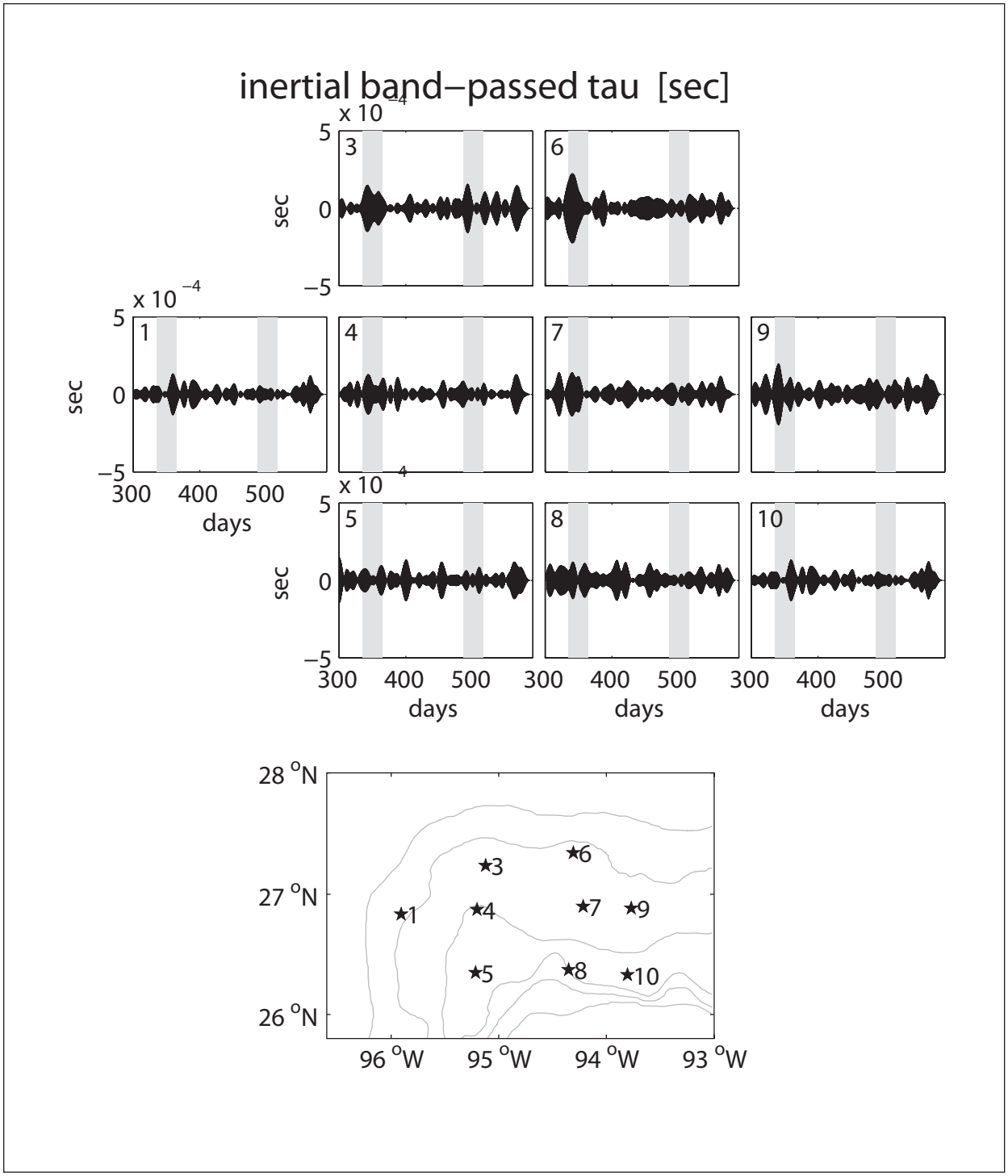

Figure 5-2. Time series of near-inertial band-passed τ in seconds plotted according to approximate geographic location. Instrument number noted in the upper left corner of each subplot. Shaded gray regions correspond to the averaging period for two case studies. Bottom panel: Bathymetry contoured every 500 m depth. PIES are denoted as stars.

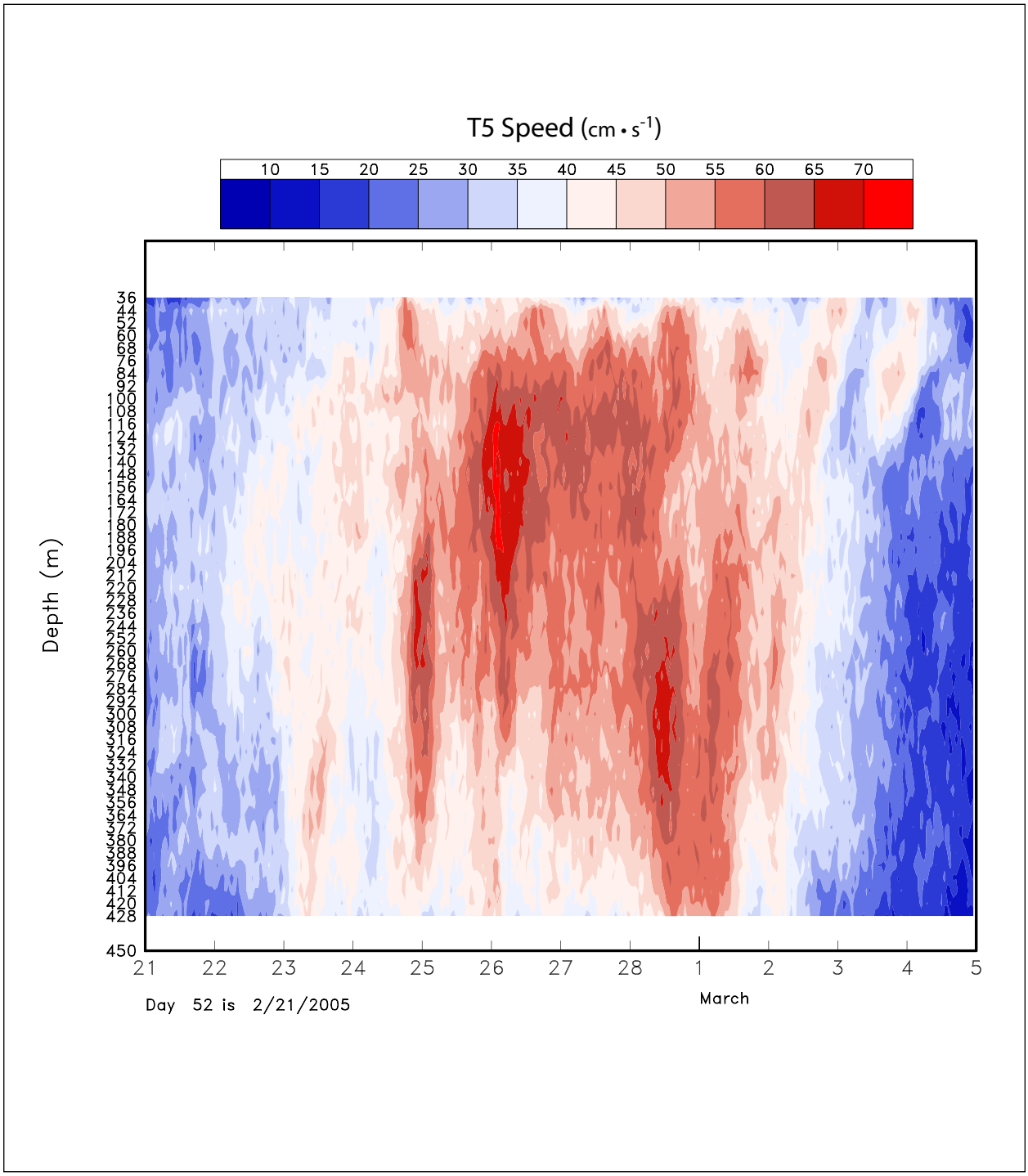

Figure 5-3. Unfiltered speed from the 450 m ADCP at T5 for the indicated interval.

CHAPTER 6 RECOMMENDATIONS

The field and remotely sensed observations acquired in support of this program's objectives provided a well-designed database with which to characterize current patterns and processes in the NW GOM during the field measurement interval. Evolving upper-layer circulation patterns and processes that were largely related to the migration and dissipation of LCEs were fairly well resolved. The resulting description and discussion helps to resolve some of the dynamic patterns associated with the LCEs as they move across the GOM, interact with other eddies and with the adjacent continental slope. The combination of fixed moorings and PIES provide compatible observations that when taken as a integrated database, allow characterization of the sequence of flow patterns that are occurring as eddies move into the NW GOM. It is of note that most of the PIES and moorings were above the Sigsbee Escarpment and hence may have been somewhat insulated from such features as TRWs that moved westward along the base of the escarpment. With this increased knowledge of current patterns, consistent and recurring kinematic features can now be more confidently resolved and described.

The documentation of high-speed jets during this study establishes increased validity of their existence – which is a significant step. Based on prior reports from the oil and gas industry, these features can have an important impact on deepwater operations. Now that they have been more confidently documented and described, they may reasonably be part of a future experimental measurement design.

As described in the Introduction to this report, the NW GOM study is one of several non-concurrent, MMS-funded measurement programs that are helping define a rational basis for the measurement locations and the spatial and temporal scales that need to be resolved. Knowledge of these scales will support design of a comprehensive study of upper and lower-layer flow patterns that are linked directly or indirectly to the LC and LCEs.

A key recommendation is for a field measurement program that includes well resolved characteristics of the LC and related LCEs and larger boundary eddies that move along the edge of the LC and LCEs. Such a study of the “source region” of many of the dynamic features that transport mass and momentum across the GOM, will provide information on a key upstream condition. In conjunction with this upstream condition, additional observations need to be made along the trajectories of eddies as they move westward and are modified as they interact with other eddies and the shoaling bathymetry of the bounding continental slope. Because the time scale of eddy shedding is 4-18 months, these coordinated measurement programs should be of sufficient duration that at least two eddy shedding cycles and subsequent translation to the western GOM are completed. This duration should, on the order of 36 months. The prior Exploratory Study in conjunction with the present study helps emphasize the significant role that the Sigsbee Escarpment has in affecting eddies and TRWs. Thus, there should be coordination of a LC study with observations further west along this important bathymetric feature.

The combined use of moored arrays supporting current measurements as well as C/T observations have proven to work effectively with PIES. In turn, the PIES and satellite altimetry are proving to be mutually consistent and hence supportive of an integrated characterization. Certainly, to date, PIES are providing important observations that are helping to establish an

appropriate method of referencing altimetric anomalies in order to define actual SSH not dependent on incorporation of long-term mean surfaces based on numerical model results. Additionally, deep Lagrangian drifters can provide unique information on total transport patterns in the deeper portions of the Gulf. Although not part of the present NW GOM study, they have provided valuable information for locating, tracking and characterizing coherent deep current patterns in the northern GOM.

CHAPTER 7 REFERENCES

Berger, T., P. Hamilton, J.J. Singer, R.R. Leben, G.H. Born, and C.A. Fox. 1996. Louisiana/Texas shelf physical oceanography program: Eddy circulation study, final synthesis report. Volume 1: Technical report. U.S. Dept. of the Interior, Minerals Management Service, Gulf of Mexico OCS Region, New Orleans, LA. OCS Study MMS 96-0051. 324 pp.

Biggs, D.C., G.S. Fargion, P. Hamilton, and R.R. Leben. 1996. Cleavage of a Gulf of Mexico Loop Current eddy by a deep water cyclone. J. Geophys. Res. 101(20):20629-20641.

DiMarco, S.F., M.K. Howard, W.D. Nowlin, Jr., and R.O. Reid. 2004. Subsurface, high-speed current jets in the deepwater region of the Gulf of Mexico: Final report. U.S. Dept. of the Interior, Minerals Management Service, Gulf of Mexico OCS Region, New Orleans, LA. OCS Study MMS 2004-022. 98 pp.

Donohue, K., P. Hamilton, K. Leaman, R. Leben, M. Prater, D.R. Watts, and E. Waddell. 2006. Exploratory study of deepwater currents in the Gulf of Mexico. Volume II: Technical report. U.S. Dept. of the Interior, Minerals Management Service, Gulf of Mexico OCS Region, New Orleans, LA. OCS Study MMS 2006-074. 430 pp.

Elliott, B.A. 1982. Anticyclonic rings in the Gulf of Mexico. J. Phys. Oceanogr. 12(11):1292-1309.

Hamilton, P. 1990. Deep currents in the Gulf of Mexico. J. Phys. Oceanogr. 20(7):1087-1104.

Hamilton, P. 2007. Deep-current variability near the Sigsbee Escarpment in the Gulf of Mexico. J. Phys. Oceanogr. 37:708-726.

Hamilton, P., T.J. Berger, J.J. Singer, E. Waddell, J.H. Churchill, R.R. Leben, T.N. Lee, and W. Sturges. 2000. DeSoto Canyon eddy intrusion study: Final report. Volume II: Technical report. U.S. Dept. of the Interior, Minerals Management Service, Gulf of Mexico OCS Region, New Orleans, LA. OCS Study MMS 2000-080. 275 pp.

Hamilton, P., J.J. Singer, E. Waddell, and K. Donohue. 2003. Deepwater observations in the northern Gulf of Mexico from in-situ current meters and PIES: Final report, Volume II: Technical report. U.S. Dept. of the Interior, Minerals Management Service, Gulf of Mexico OCS Region, New Orleans, LA. OCS Study MMS 2003-049. 95 pp.

Kirwan, A.D., Jr., W.J. Merrell, Jr., J.K. Lewis, and R.E. Whitaker. 1984. Lagrangian observations of an anticyclonic ring in the western Gulf of Mexico. J. Geophys. Res. 89(C3):3417-3424.

Leben, R.R. 2005. Altimeter-derived Loop Current metrics. In: Sturges, W. and A. Lugo-Fermandez, eds. Circulation in the Gulf of Mexico: observations and models, Geophysical Monograph 161. American Geophysical Union, Washington, DC. pp. 181-201.

Lewis, J.K. and A.D. Kirwan, Jr. 1985. Some observations of ring topography and ring-ring interactions in the Gulf of Mexico. J. Geophys. Res. 90(C5):9017-9028.

Nowlin, W.D., Jr., A.E. Jochens, S.F. DiMarco, R.O. Reid, and M.K. Howard. 2001. Deepwater physical oceanography reanalysis and synthesis of historical data: Synthesis report. U.S. Dept. of the Interior, Minerals Management Service, Gulf of Mexico OCS Region, New Orleans, LA. OCS Study MMS 2001-064. 530 pp.

Sturges, W. and R. Leben. 2000. Frequency of ring separations from the Loop Current in the Gulf of Mexico: A revised estimate. J. Phys. Oceanogr. 30(7):1814-1819.

The Department of the Interior Mission

As the Nation's principal conservation agency, the Department of the Interior has responsibility for most of our nationally owned public lands and natural resources. This includes fostering sound use of our land and water resources; protecting our fish, wildlife, and biological diversity; preserving the environmental and cultural values of our national parks and historical places; and providing for the enjoyment of life through outdoor recreation. The Department assesses our energy and mineral resources and works to ensure that their development is in the best interests of all our people by encouraging stewardship and citizen participation in their care. The Department also has a major responsibility for American Indian reservation communities and for people who live in island territories under U.S. administration.

The Minerals Management Service Mission

As a bureau of the Department of the Interior, the Minerals Management Service's (MMS) primary responsibilities are to manage the mineral resources located on the Nation's Outer Continental Shelf (OCS), collect revenue from the Federal OCS and onshore Federal and Indian lands, and distribute those revenues.

Moreover, in working to meet its responsibilities, the **Offshore Minerals Management Program** administers the OCS competitive leasing program and oversees the safe and environmentally sound exploration and production of our Nation's offshore natural gas, oil and other mineral resources. The MMS **Minerals Revenue Management** meets its responsibilities by ensuring the efficient, timely and accurate collection and disbursement of revenue from mineral leasing and production due to Indian tribes and allottees, States and the U.S. Treasury.

The MMS strives to fulfill its responsibilities through the general guiding principles of: (1) being responsive to the public's concerns and interests by maintaining a dialogue with all potentially affected parties and (2) carrying out its programs with an emphasis on working to enhance the quality of life for all Americans by lending MMS assistance and expertise to economic development and environmental protection.